

# NAVAL POSTGRADUATE SCHOOL MONTEREY, CALIFORNIA



## THESIS

**LINEAR STRUCTURAL STRESS ANALYSIS OF A  
HULL GIRDER PENETRATION AND A SHORT  
LONGITUDINAL BULKHEAD USING FINITE  
ELEMENT MODELING**

by

Gregg W. Baumann

June, 1997

Thesis Advisor:

Charles N. Calvano

19971029 145

Approved for public release; distribution is unlimited.

UNCLASSIFIED

# REPORT DOCUMENTATION PAGE

Form Approved OMB No. 0704-0188

Public reporting burden for this collection of information is estimated to average 1 hour per response, including the time for reviewing instruction, searching existing data sources, gathering and maintaining the data needed, and completing and reviewing the collection of information. Send comments regarding this burden estimate or any other aspect of this collection of information, including suggestions for reducing this burden, to Washington Headquarters Services, Directorate for Information Operations and Reports, 1215 Jefferson Davis Highway, Suite 1204, Arlington, VA 22202-4302, and to the Office of Management and Budget, Paperwork Reduction Project (0704-0188) Washington DC 20503.

1. AGENCY USE ONLY ( <i>Leave blank</i> )	2. REPORT DATE June 1997	3. REPORT TYPE AND DATES COVERED Master's Thesis	
4. TITLE AND SUBTITLE: LINEAR STRUCTURAL STRESS ANALYSIS OF A HULL GIRDER PENETRATION AND A SHORT LONGITUDINAL BULKHEAD USING FINITE ELEMENT MODELING		5. FUNDING NUMBERS	
6. AUTHOR(S) Gregg W. Baumann		8. PERFORMING ORGANIZATION REPORT NUMBER	
7. PERFORMING ORGANIZATION NAME(S) AND ADDRESS(ES) Naval Postgraduate School Monterey CA 93943-5000		10. SPONSORING/MONITORING AGENCY REPORT NUMBER	
9. SPONSORING/MONITORING AGENCY NAME(S) AND ADDRESS(ES)		11. SUPPLEMENTARY NOTES The views expressed in this thesis are those of the author and do not reflect the official policy or position of the Department of Defense or the U.S. Government.	
12a. DISTRIBUTION/AVAILABILITY STATEMENT Approved for public release; distribution is unlimited.		12b. DISTRIBUTION CODE	
13. ABSTRACT ( <i>maximum 200 words</i> ) <p>The objective of this study is to investigate structural shadow zones encountered in shipbuilding design using the I-DEAS<sup>TM</sup> (Integrated Design Engineering Analysis Software) software. The term "shadow zone" refers to areas of low stress concentrations that are caused by lines of stress bending around structural discontinuities. Two ship design situations frequently encountered that result in shadow zones are hull girder penetrations and short structural longitudinal bulkheads. In both of these situations, a long-used rule of thumb is to construct a line with a slope of 1:4 originating from the discontinuity that encompasses the area of low stress. The material within this line is then considered ineffective when computing the section modulus. This can prove to be expensive. However, powerful finite element analysis software is readily available that can analyze the shadow zones in greater detail and possibly minimize the area considered ineffective. This study uses the I-DEAS<sup>TM</sup> software to develop finite element models of the cited design situations for a U.S. Navy Frigate, FFG-7 class of ship. It conducts a static structural linear analysis of the ship balanced on a trochoidal wave of height <math>1.1\sqrt{L}</math>. The results generated in this study validate the rule of thumb in both situations.</p>			
14. SUBJECT TERMS Shadow Zone, Finite Element Modeling, Hull Girder Discontinuities		15. NUMBER OF PAGES 60	
		16. PRICE CODE	
17. SECURITY CLASSIFICATION OF REPORT Unclassified	18. SECURITY CLASSIFICATION OF THIS PAGE Unclassified	19. SECURITY CLASSIFICATION OF ABSTRACT Unclassified	20. LIMITATION OF ABSTRACT UL

NSN 7540-01-280-5500

Standard Form 298 (Rev. 2-89)  
Prescribed by ANSI Std. Z39-18 298-102



Approved for public release; distribution is unlimited.

**LINEAR STRUCTURAL STRESS ANALYSIS OF A HULL GIRDER  
PENETRATION AND A SHORT LONGITUDINAL BULKHEAD USING  
FINITE ELEMENT MODELING**

Gregg W. Baumann  
Lieutenant, United States Navy  
B.S., Clarkson University, 1986

Submitted in partial fulfillment  
of the requirements for the degree of

**MASTER OF SCIENCE IN MECHANICAL ENGINEERING**

from the

**NAVAL POSTGRADUATE SCHOOL**

**June 1997**

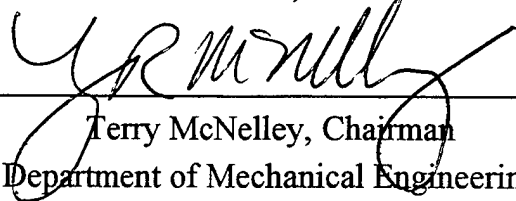
Author:

  
Gregg W. Baumann

Approved by:



Charles N. Calvano, Thesis Advisor

  
Terry McNelley, Chairman  
Department of Mechanical Engineering

• • • • •

## ABSTRACT

The objective of this study is to investigate structural shadow zones encountered in shipbuilding design using the I-DEAS<sup>TM</sup> (Integrated Design Engineering Analysis Software) software. The term "shadow zone" refers to areas of low stress concentrations that are caused by lines of stress bending around structural discontinuities. Two ship design situations frequently encountered that result in shadow zones are hull girder penetrations and short structural longitudinal bulkheads. In both of these situations, a long-used rule of thumb is to construct a line with a slope of 1:4 originating from the discontinuity that encompasses the area of low stress. The material within this line is then considered ineffective when computing the section modulus. This can prove to be expensive. However, powerful finite element analysis software is readily available that can analyze the shadow zones in greater detail and possibly minimize the area considered ineffective. This study uses the I-DEAS<sup>TM</sup> software to develop finite element models of the cited design situations for a U.S. Navy Frigate, FFG-7 class of ship. It conducts a static structural linear analysis of the ship balanced on a trochoidal wave of height  $1.1\sqrt{L}$ . The results generated in this study validate the rule of thumb in both situations.



## TABLE OF CONTENTS

I. INTRODUCTION .....	1
A. BACKGROUND .....	1
B. SELECTED HULL FOR MODELING .....	3
C. ANALYSIS OF BENDING AND SHEAR STRESSES FOR MODEL .....	5
II. MODEL DEVELOPMENT .....	11
A. DESCRIPTION OF MODELING SOFTWARE .....	11
B. DESCRIPTION OF THE GEOMETRIC MODEL DEVELOPMENT .....	13
III. FINITE ELEMENT MODEL DEVELOPMENT .....	17
A. DESCRIPTION OF GEOMETRIC MODELING .....	17
B. MESHING OF MODELS .....	19
C. BOUNDARY CONDITIONS .....	23
IV. RESULTS .....	33
A. HULL GIRDER PENETRATION MODEL .....	33
B. LONGITUDINAL BULKHEAD MODEL .....	38
C. MODELING PROCEDURES .....	41
V. CONCLUSIONS .....	45
LIST OF REFERENCES .....	47
INITIAL DISTRIBUTION LIST .....	49



## ACKNOWLEDGEMENTS

I thank Professor Calvano for his assistance and guidance throughout my thesis endeavor. His dedicated efforts assisted me in both learning beyond what I knew before I started and in guiding me towards achievable goals. In addition, I thank Professor Gordis for his assistance with I-DEAS<sup>TM</sup> and his insightful recommendations. His recommendations were invaluable in the sound development of the finite element models.

I thank my parents for instilling in me the necessary drive and dedication that is necessary in completing a task of this magnitude. Finally, I thank my wife, JoAnn, for her never-ending support throughout my thesis endeavor and my Master's degree. Her constant encouragement and understanding made the completion of this thesis possible.

# I. INTRODUCTION

## A. BACKGROUND

The phrase "shadow zone" has long been recognized for employing various rules of thumb for stress analyses in preliminary ship designs. It refers to areas of relatively low stress concentration when compared to surrounding material. The types of situations that result in "shadow zones" are numerous. However, two situations of particular interest that are encountered frequently are hull girder penetrations and short longitudinal structural bulkheads. The shadow zones created in these circumstances cause ship designers to include extra structural material in a hull girder design to obtain an acceptable section modulus. It is these two circumstances that this study investigates.

Shadow zones, or areas of low stress concentrations, in the two circumstances cited are the result of the lines of force bending around a structural discontinuity. In the case of a hull penetration where the bending stress trajectories are parallel to the long edge of the hole, the lines of force must bend around the transverse edges. In order for the static forces to remain in equilibrium, they must be distributed to regions of the material which can provide an equal and opposite reaction. The reason that the forces have to bend around the penetration is that an equal and opposite force can not be provided at the transverse edge. Hence, lines of force bend around the penetration causing an area of low stress concentration immediately fore and aft of the hole.

The shadow zones resulting from a short longitudinal bulkhead can be explained by an argument similar to that of the hull penetration. For a short longitudinal bulkhead, it is assumed that the only points on the fore or aft ends of the bulkhead that can transmit force in the longitudinal direction are at the attachment points in corners. The reason for this is that there is no adjacent structural material in the longitudinal direction fore or aft of the vertical edges to provide a reaction. Hence, the lines of stress emanate and fan out from the corners of the bulkhead causing low stress levels adjacent to the vertical edges.

In typical ship designs, penetrations for such things as personnel access and ventilation ducting are made through structural material considered to be part of the hull girder. In such cases, the Naval Sea Systems Command (NAVSEA), the Ship Structure Committee (SSC), and other ship design related activities typically employ a rule of thumb which states, "Material to be considered longitudinally effective...is material starting in the shell or in continuous decks into which stress can 'flow' without deviating from the fore-aft direction by more than a slope of 4:1 (longitudinal units over transverse units)" [Ref. 1]. Figure 1 depicts the areas considered to be ineffective. NAVSEA is the primary ship design and acquisition activity for the U.S. Navy. The SSC is an interagency body that supports its members by promoting safety, economy, education, and marine environmental protection in the North American Maritime industry through the advancement of marine structures technology.

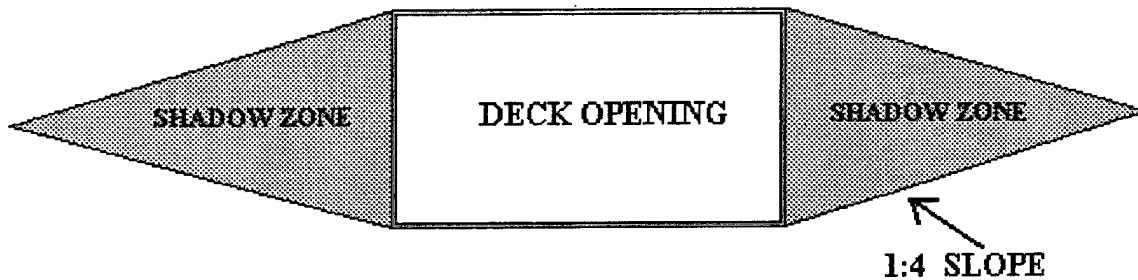


FIGURE 1. Deck opening with fore and aft shadow zones

In the case of short structural longitudinal bulkheads, a shadow zone is also cast. In this circumstance, the NAVSEA rule of thumb states, "Shadow areas adjacent to discontinuities such as the ends of longitudinal bulkheads, strength decks, and inner bottoms, are bounded by lines with a 1:4 slope." Figure 2 depicts the ineffective area. [Ref. 2]

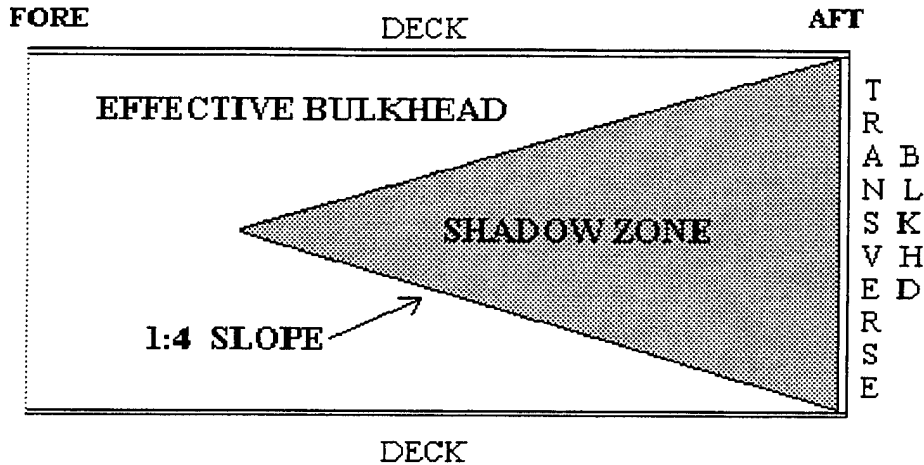


FIGURE 2. Short longitudinal bulkhead intersecting a transverse bulkhead.

The ineffective areas are important when calculating acceptable section moduli in way of these areas. The procedure is to neglect the contributions of the material in the areas defined by the rules of thumb when calculating the section modulus. The rules of thumb apply for longitudinal bending of the ship's hull in both the hogging and sagging condition and are based upon basic beam bending theory. Basic beam bending theory assumes that plane sections remain plane after bending in the elastic range.

The rules of thumb were developed prior to the availability of today's powerful finite element analysis (FEA) software. In addition, some consider them to be overly conservative. In response, the SSC has solicited research input on recent analyses in this area. The idea for this thesis originated from this request. It is the purpose of this thesis to further investigate the shadow zones created during longitudinal bending of the ship's hull girder using currently available and more powerful finite element software.

## B. SELECTED HULL FOR MODELING

In order to obtain reasonable and reliable data, the development of a realistic model is required for conducting an FEA. Development of a model based on an existing

hull form is preferred over that of a proposed design. The use of an existing hull allows for access to a larger data base of information and allows for comparisons against existing data where appropriate. Based on this, the U.S. Navy Oliver Hazard Perry Class Guided Missile Frigate (FFG-7) ship was chosen as the baseline for a model development. The principal characteristics of the FFG-7 are listed in Table 1.

Displacement - full load	4100 tons
Length	445 ft.
Beam	45 ft.
Draft	14.8 ft.
Speed	29 kts.
Range	4500 NM @ 20 kts.
Main Machinery	2 GE LM 2500 Gas Turbines Engines
Shafts	Single CPP

Table 1. Principal characteristics of U.S. Navy Oliver Hazard Perry Class Guided Missile Frigate (FFG-7) ship

Specific ship data was obtained from information provided in reference [2]. The information obtained included ship scantlings, moments of inertia, curves of weight, shear, and bending moment for a FFG-7 class ship balanced on a trochoidal wave. In addition, information regarding resulting bending stresses was also obtained. The information presented in reference [2] was obtained directly from actual ship plans, drawings, specifications, and ship data. Hence, it's accuracy was considered sufficient for the detail necessary in this study. It is this data that was used as the basis for this thesis' model development.

Although the FFG-7 Class of ship was built in the 1970's, its structural design is similar to today's naval warship construction. Hence, results of structural analyses obtained from this warship will be reliable and applicable to today's designs. In addition, the type of information being sought with this study can be easily applied to commercial ship building designs without appreciable loss of accuracy. Overall, the U.S. Navy Oliver

Hazard Perry Class Guided Missile Frigate (FFG-7) ship provides an excellent baseline for a model development for this study.

### **C. ANALYSIS OF BENDING AND SHEAR STRESSES FOR MODEL**

Traditional ship design assumes the hull behaves as a built-up box girder that behaves in accordance with simple beam bending theory. The built-up box girder, more commonly referred to as the hull girder, is subject to downward forces of weight from the weight of the ship and its contents and the upward forces of buoyancy. The combination of the downward and buoyancy forces creates shearing forces along the length of the hull. The net result is an induced bending moment that, when analyzed, behaves similar to that of a simple beam.

Simple beam flexure theory makes the following assumptions for stress analysis in bending [Ref. 3].

- The beam is prismatic.
- The beam length is at least 10 times its depth.
- External forces act at right angles to the beam and in a plane of symmetry.
- Flexure is slight and stresses are within the elastic limit.
- The beam is constructed of a homogeneous material that obeys Hooke's law and whose tensile and compressive moduli are equal.
- Every layer is free to expand and contract laterally and longitudinally as if separate from other layers.
- Plane sections remain plane after flexure.

Although a ship's hull does not rigorously conform to the above assumptions, it does closely approximate them. It is close enough that simple beam flexure theory has long been employed, yielding serviceably accurate results. A ship's hull design is very complex and an analysis otherwise would be extremely complex and costly. The approximations in

most cases give results which, when coupled with previous history, can be effectively applied to a design. The purpose of presenting these assumptions and theory is not to prove or disprove their validity, but rather to provide an understanding for the development of this study's model.

A ship's hull structural response can be categorized in three different areas [Ref. 4].

- Primary response: The response of the entire hull due to bending caused by a longitudinal distribution of load and buoyancy.
- Secondary response: The response of major substructures or definable areas of the hull such as bulkheads.
- Tertiary response: The response of minor substructures due to very localized loads.

The focus of this work is on the primary response of a ship's hull. Since secondary and tertiary responses can vary significantly from one design to another, the results of this analysis would be more generically applicable by omitting them. Furthermore and most importantly, by restricting the model to primary responses only, the effect of longitudinal bending on shadow zones can be isolated.

An analysis of the primary response of the hull girder while incorporating simple beam flexure theory begins by identifying the distributed weight of the ship and its contents and the buoyant forces on the hull. These forces are added to obtain the hull loading. The loading is integrated along the length of the ship to obtain the resulting bending moment as a function of the length. Equations (1-4) are the expressions for obtaining the shear and bending moment from the loading.

$$P = \frac{dS}{dx} \qquad \text{Equation (1)}$$

$$S = \int P dx \quad \text{Equation (2)}$$

$$S = \int \frac{dM}{dx} \quad \text{Equation (3)}$$

$$M = \int S dx = \iint P dx \quad \text{Equation (4)}$$

where:

$P$  = loading

$S$  = shear

$M$  = bending moment

In order to determine the bending stress in the hull, the section modulus must first be determined. This is calculated from Equation (5). Bending stress is then found from the flexure formula, Equation (6).

$$SM = \frac{I}{c} \quad \text{Equation (5)}$$

$$\sigma = \frac{M}{SM} \quad \text{Equation (6)}$$

where:

$SM$  = section modulus

$I$  = moment of inertia of the section about the neutral axis

$c$  = distance from the neutral axis

$\sigma$  = bending stress

Hull deflection and the slope can also be determined from the loading and simple beam flexure theory. Slope is a function of the third integral of load with respect to length divided by EI, Equation (7).

$$\theta = \frac{1}{EI} \int M dx = \frac{1}{EI} \iiint P dx \quad \text{Equation (7)}$$

where:

$\theta$  = slope

$E$  = Young's modulus of elasticity

Hull deflection is determined from the double integration of the bending moment or the fourth integral of load with respect to length divided by EI, Equation (8).

$$v = \frac{1}{EI} \iint M dx = \frac{1}{EI} \iiint \int P dx \quad \text{Equation (8)}$$

For some specific applications an alternative method for determining hull girder deflection is by using semi-empirical approximations. This method is discussed in greater depth in the Boundary Conditions section of this paper.

Since ship motion on the sea is extremely complex and dynamic, a standard method for analyzing and comparing structural analyses is to place a momentarily still ship on a wave [Ref. 5]. The ship is assumed to be balanced and without velocity and acceleration with respect to the wave. In this condition, the curves of weight and buoyancy are determined, followed by subsequent integrations to obtain the bending stress. A standard wave used for comparison purposes is a trochoidal wave. This wave shape is formed by picking a point at a radius  $r$  within a circle and rolling that circle along

a horizontal plane. The shape generated from the point at radius  $r$  is considered to be a trochoidal shape. A commonly used wave height is  $1.1\sqrt{L}$  where  $L$  is the ship's length in feet.

There are many alternative methods for conducting hull girder structural analyses. However, the method presented here is commonly accepted and one which can be employed with relative ease while still obtaining realistic results. It is presented here to provide an understanding of the development of this study's model.



## II. MODEL DEVELOPMENT

### A. DESCRIPTION OF MODELING SOFTWARE

The use of finite element modeling (FEM) and finite element analysis (FEA) is widespread in the marine, aircraft, and other design intensive industries. FEM is associated with generating a mathematical model of a physical part by breaking it into discrete sections called elements. In using FEM, the exact physical dimensions may or may not be used. Depending on the analysis and the intricacies of the part, some level of detail may be omitted. This does not necessarily lead to errors in the results since the focus of the analysis may not be greatly dependent on the fine details of the part. FEA is dependent on FEM in that it takes the mathematical model and applies a systematic set of governing equations to it. The set of equations is used to approximate the displacements of the nodes within the elements. The set of equations can be related to such fields as structural, fluid flow, heat transfer, or dynamic response analyses.

Many different software packages for conducting FEM and FEA are available. The general procedures for conducting an analysis are essentially the same for the different packages. However, some of the software packages have better procedures for conducting certain specific types of analyses over others or have better associated modeling packages, depending on the application. For this study, the software used was I-DEAS<sup>TM</sup> (Integrated Design Engineering Analysis Software). It is written by Structural Dynamics Research Corporation (SDRC). I-DEAS<sup>TM</sup> is a fully integrated finite element solver that accomplishes both FEM and FEA. The software provides the means for conducting preprocessing, solving, and post-processing. Although it has many different applications, the only application necessary for this model was the linear static structural analysis package.

In solving a linear static structural analysis, I-DEAS™ generates a stiffness equation for each element in the model, Equation (9) [Ref. 6].

$$\{f_1\} = [k_1]\{d_1\}, \{f_2\} = [k_2]\{d_2\}, \dots, \quad \text{Equation (9)}$$

where:

$[k]$  = element stiffness matrix

$\{d\}$  = nodal degree of freedom, displacement

$\{f\}$  = force vector

The element stiffness equations are collected and a global stiffness matrix is generated. The result is a system governing matrix equation for a linear static structural analysis, Equation (10).

$$\{F\} = [K]\{D\} \quad \text{Equation (10)}$$

The nodal displacements are solved for in Equation (11) by applying appropriate boundary conditions to the system force vector.

$$\{D\} = [K]^{-1}\{F\} \quad \text{Equation (11)}$$

The number of matrix equations to be solved depends upon the types of elements utilized and the number of discrete sections in the model. In solving this system of equations, I-DEAS™ supports eleven different families of elements for structural analyses and an unlimited number of equations [Ref. 7]. The only major potential limiting factor in applying I-DEAS™ to a static structural analysis is the processing capability of the hardware on which it is run. The type of hardware used in this analysis was a Silicon Graphics operating system.

## B. DESCRIPTION OF THE GEOMETRIC MODEL DEVELOPMENT

Since the shadow areas under consideration in this study were being analyzed independently, they necessitated two independent finite element models. The first model incorporated a section of the FFG-7 hull with a standard size personnel access hole cut in the hull girder. The second model utilized the same section of the FFG-7 hull without the access cut, but included a longitudinal structural bulkhead. In order to isolate the effects on the stress flow in the section caused by the access cut and the bulkhead, the only material included were continuous structural members that comprised the hull girder. Application specific items such as equipment foundations, piping penetrations, ventilation ducts, and other similar hull girder disruptions were not included. This was done in order to isolate the effects around the structure in question and to keep the results generically applicable to different designs. Figure 3 depicts the hull girder cross section at station 10 with the structural component dimensions listed in Table 2.

The section of hull used from the FFG-7 was station 10 out of 20 stations. This section was modeled since the maximum bending moment from a trochoidal wave on the Frigate hull is in this area. Since most large combatants and tankers maintain a similar hull shape around their midbody, the model was developed assuming the scantlings at station 10 remained constant over the length of the section modeled. The length of section used in both cases was 30 feet. This ensured there was sufficient material fore and aft of the access cut and sufficient bulkhead material to avoid the effects of the discrete nodal boundary conditions.

Since the hull is symmetric about the longitudinal axis and the only forces considered were those causing longitudinal bending, only half of the section at station 10 required modeling. An appropriate restraint was applied to the model to represent the reaction forces created by the other half of the section. By doing this the size of the numerical model is cut in half which frees up computer hardware memory. The advantage

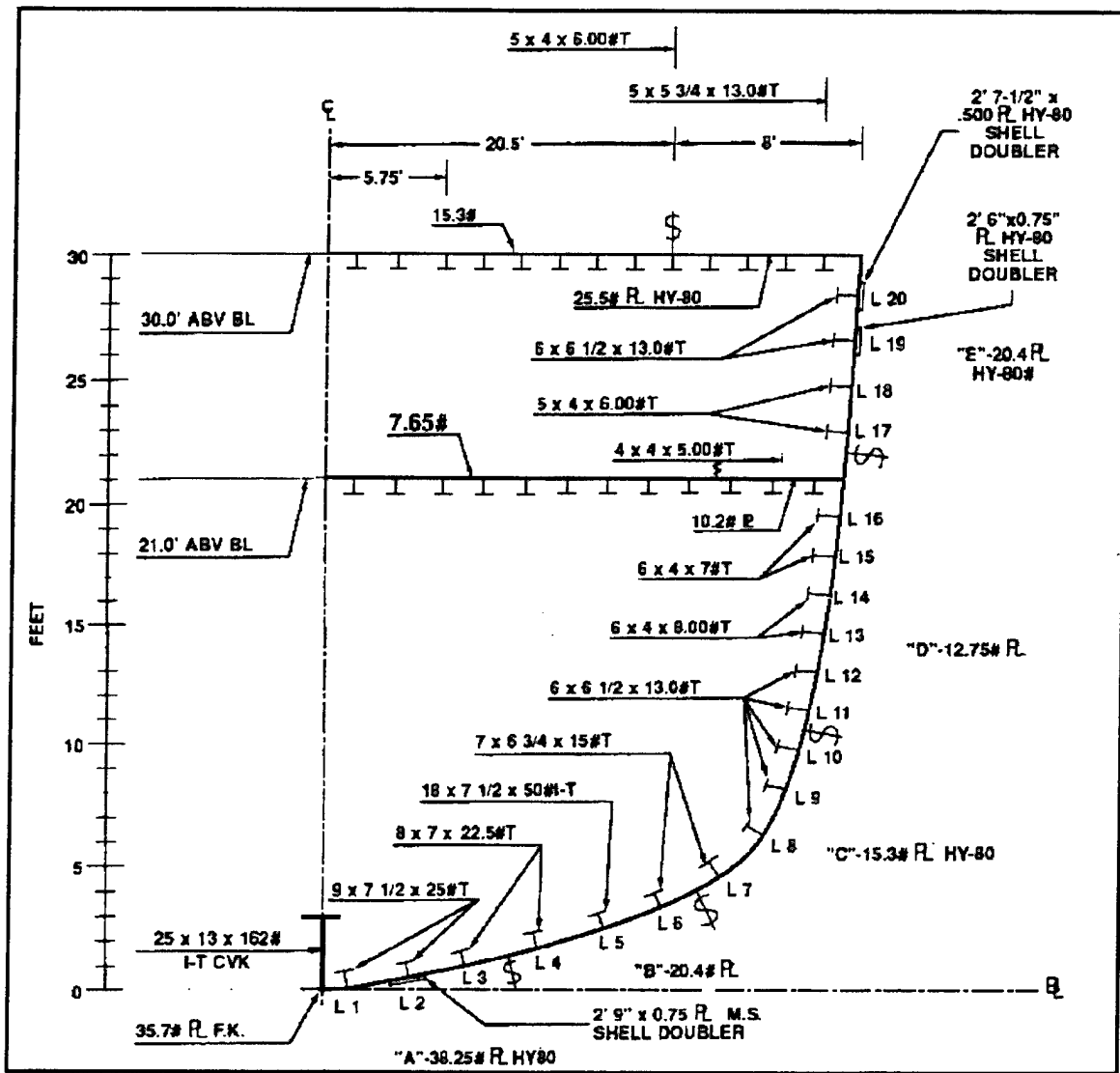


FIGURE 3. FFG-7 Hull Girder Cross Section at Station 10

COMPONENT	DIMENSIONS
	(inches)
Mn Dk Girders, Inbd (7) -T	5 x 4 x 6#
Mn Dk Girders, Outbd (4) - T	5 x 5.75 x 13#
2 <sup>nd</sup> Dk Girders, (10) - T	4 x 4 x 5#
Mn Dk Plating, Inbd	246 x 0.375
Mn Dk Plating, Outbd	84x .625
2 <sup>nd</sup> Dk Plating, Inbd	225 x .25
2n Dk Plating, Outbd	51 x .25
"E" Strake	93 x .3125
"D" Strake	162 x .3125
"C" Strake	84 x .375
"B" Strake	93.25 x .5
"A" Strake	96 x .75
"E" Doubler, upper	31.5 x .5
"E" Doubler, lower	30 x .75
"A" Doubler	33 x .75
<b>Side Stringers</b>	
L20 - T	6 x 6 x 13#
L19 - T	6 x 6 x 13#
L18 - T	5 x 4 x 6#
L17 - T	5 x 4 x 6#
L16 - T	6 x 4 x 7#
L15 - T	6 x 4 x 7#
L14 - T	6 x 4 x 8#
L13 - T	6 x 4 x 8#
L12 - T	6 x 6.5 x 13#
L11 -T	6 x 6.5 x 13#
L10 - T	6 x 6.5 x 13#
L9 - T	6 x 6.5 x 13#
L8 - T	6 x 6.5 x 13#
<b>Bottom Longitudinals</b>	
L7 - T	7 x 6.75 x 15#
L6 - T	7 x 6.75 x 15#
L5 - I - T	18 x 7.5 x 50#
L4 - T	8 x 7 x 22.5#
L3 - T	8 x 7 x 22.5#
L2 - T	9 x 7.5 x 25#
L1 - T	9 x 7.5 x 25#
CVK (1/2) I - T	25 x 13 x 162#
Flat Keel (1/2)	14 x .875

Table 2. FFG-7 Hull Section Structural Dimensions at Station 10

this provided was the ability to refine the finite element mesh around the areas of interest for better accuracy.

The first model generated was for the case of the personnel access cut. The cut for the hatchway was placed in the fore and aft direction along the centerline of the hull in the main deck. A standard size hatchway of 30 inches by 60 inches was used. However, since it was placed along the centerline only half of the width was necessary. The radii used for the corners were  $1/4$  of the length of the hatchway's transverse dimension. This conforms to standard U.S. Naval warship specifications for installations amidships in the middle  $3/5$  of the ship. [Ref. 8] Since hatch coamings are not used in all applications, they were omitted in this study. This helped in keeping the results more generically applicable.

The second model generated was for the case of the longitudinal structural bulkhead. The bulkhead was placed parallel to the centerline but was offset approximately 13 feet towards the centroid of the half section. It was not placed exactly on the centroid since it would have interfered with a deck girder. The bulkhead is affixed between the main and first deck and runs the length of the section. It is constructed of medium steel and has a material thickness of 0.25 inches. The assumption was made that the bulkhead ended on either end of the section and abutted some form of transverse member. It was further assumed to be welded in place without the aid of reinforcement plates. Again, this was done to keep the results generically applicable.

### III. FINITE ELEMENT MODEL DEVELOPMENT

#### A. DESCRIPTION OF GEOMETRIC MODELING

The specific application used within I-DEAS<sup>TM</sup> for the finite element model generation was the "Simulation" software. This application offers a broad set of tools for building geometry and finite element models, analyzing models, and evaluating results for static structural analyses. Within "Simulation", there were seven specific tasks utilized to construct and analyze the models in this study. The tasks and their function are listed in Table 3.

TASK	FUNCTION
Master Modeler	Construct the geometric model
Master Surfacing	Construct the geometric model
Boundary Conditions	Apply forces, constraints, restraints to model
Meshing	Breaks model into discrete elements and nodes
Beam Section	Utilizes beam elements to represent structural members
Model Solution	Solves the system of matrix equations
Post Processing	Displays results of the solutions to the model

Table 3. Tasks within the I-DEAS Simulation Application and Their Function.

Each model was developed by sequentially accomplishing the tasks using the standard FEM approach. Figure 4 is a flowchart illustrating the sequential procedures followed.

The geometry of each model was developed from the section view in Figure 3 using the Master Modeler/Surfacing tasks within I-DEAS<sup>TM</sup>. The hull offsets and deck locations were matched to the actual structural design. Longitudinal reinforcing, the "T" and "I" beams, were included in the model since these are also assumed to comprise the hull girder. The hull section was input by constructing a solid geometry and then defining

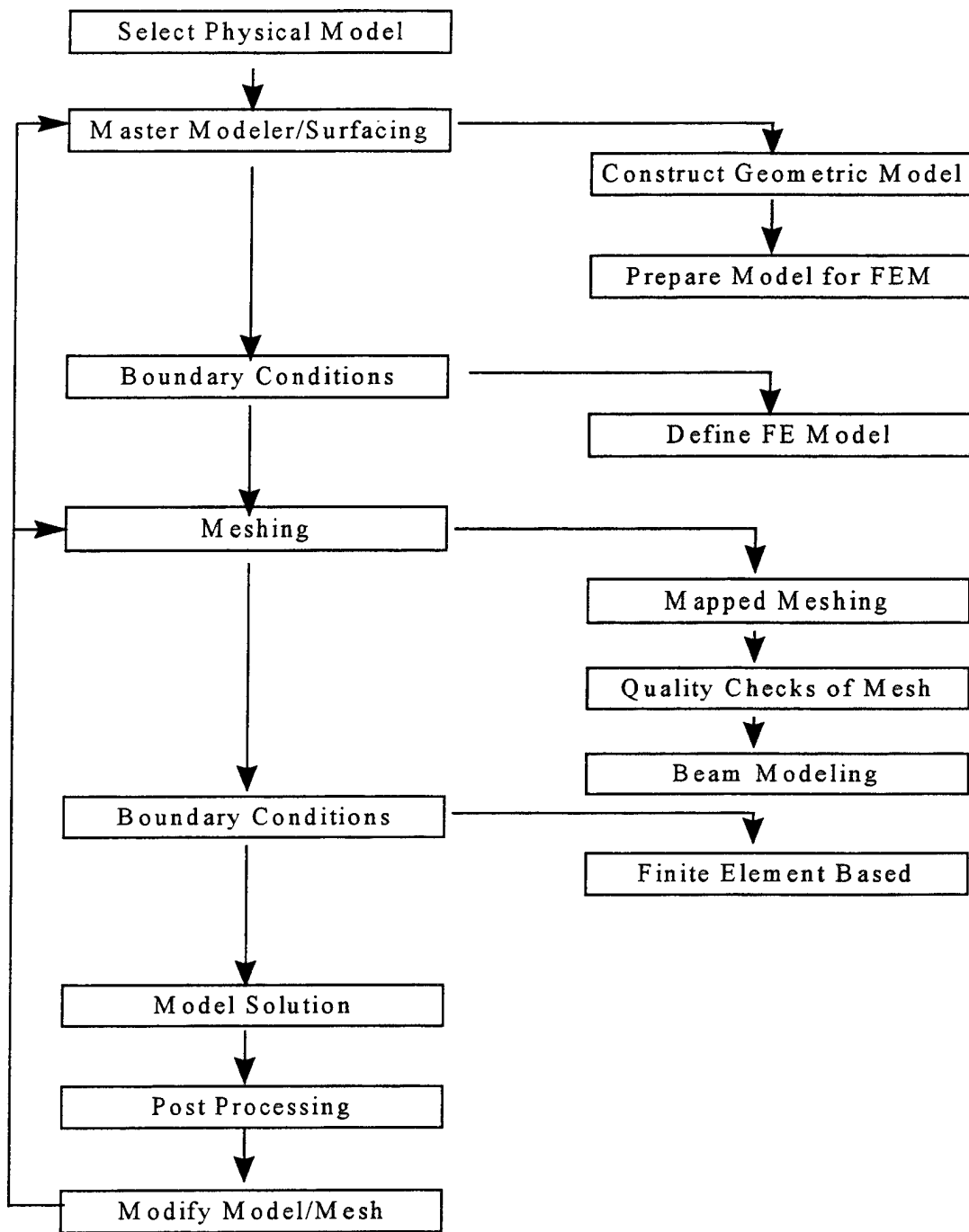


FIGURE 4. Flow Chart for Model Development, Analysis, and Post Processing

surfaces in areas where plating and longitudinals were to be placed. The size of each surface was determined by where plating thickness changed, plating material changed, and where longitudinals were welded to the structure. Designating separate surfaces simplified the meshing procedures and aided in matching the physical properties of the model to the actual structure. Reference planes were also used to properly orient the longitudinals to the hull. Figures 5 and 6 show the geometry of the hull penetration and longitudinal bulkhead models respectively. Reference planes and designated surfaces are included in the figures.

## **B. MESHING OF MODELS**

The geometric models were broken up into discrete finite elements by accomplishing mapped meshing on each surface. This was done using the meshing task within I-DEAS. Mapped meshing is a procedure whereby the user inputs the number of desired elements per surface boundary. This procedure was used over free meshing since it gives the user much greater control over the mesh density. Free meshing allows the computer software to generate the entire mesh while restricting some of the user's abilities to control the mesh density. Manual meshing was not necessary in either model since each geometry was clearly defined. Furthermore, manual meshing is a time intensive operation for large models since it requires the user to manually input the nodes and define each element.

All the plating within the hull was modeled using thin shell linear quadrilateral and triangular elements. In general, thin shell elements are used most effectively in structures with relatively thin walls as compared to their other dimensions and where bending and in-plane forces are important [Ref. 9]. Using thin shell elements assumes that stress can only vary linearly through the thickness of the material. Thin shell elements offer six degrees of freedom per node, three each in rotation and translation. Visually, the element is two dimensional, however the software stores the thickness of each element and uses it during

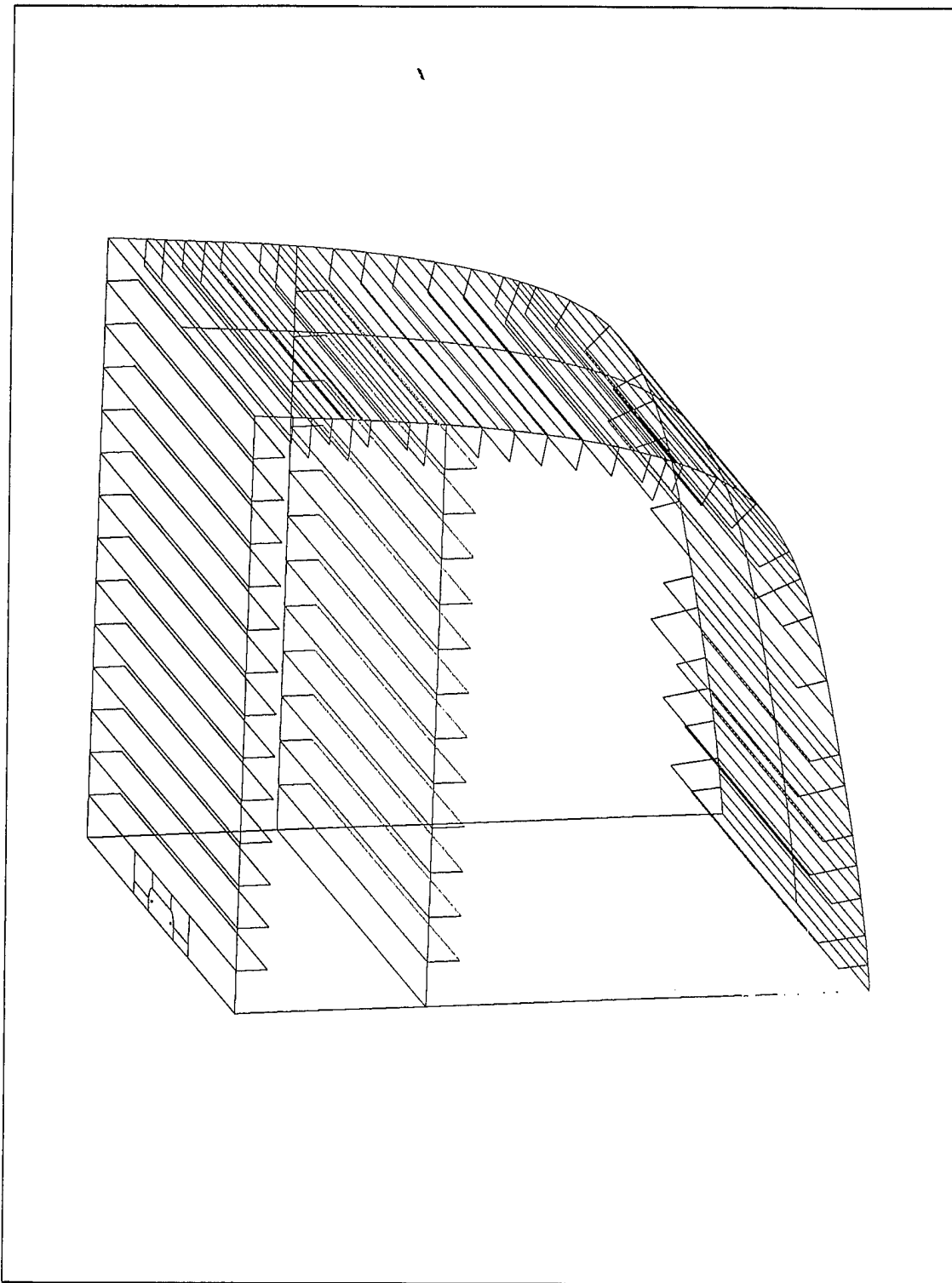


FIGURE 5. View of the Hull Penetration Model's Surfaces and Reference Planes

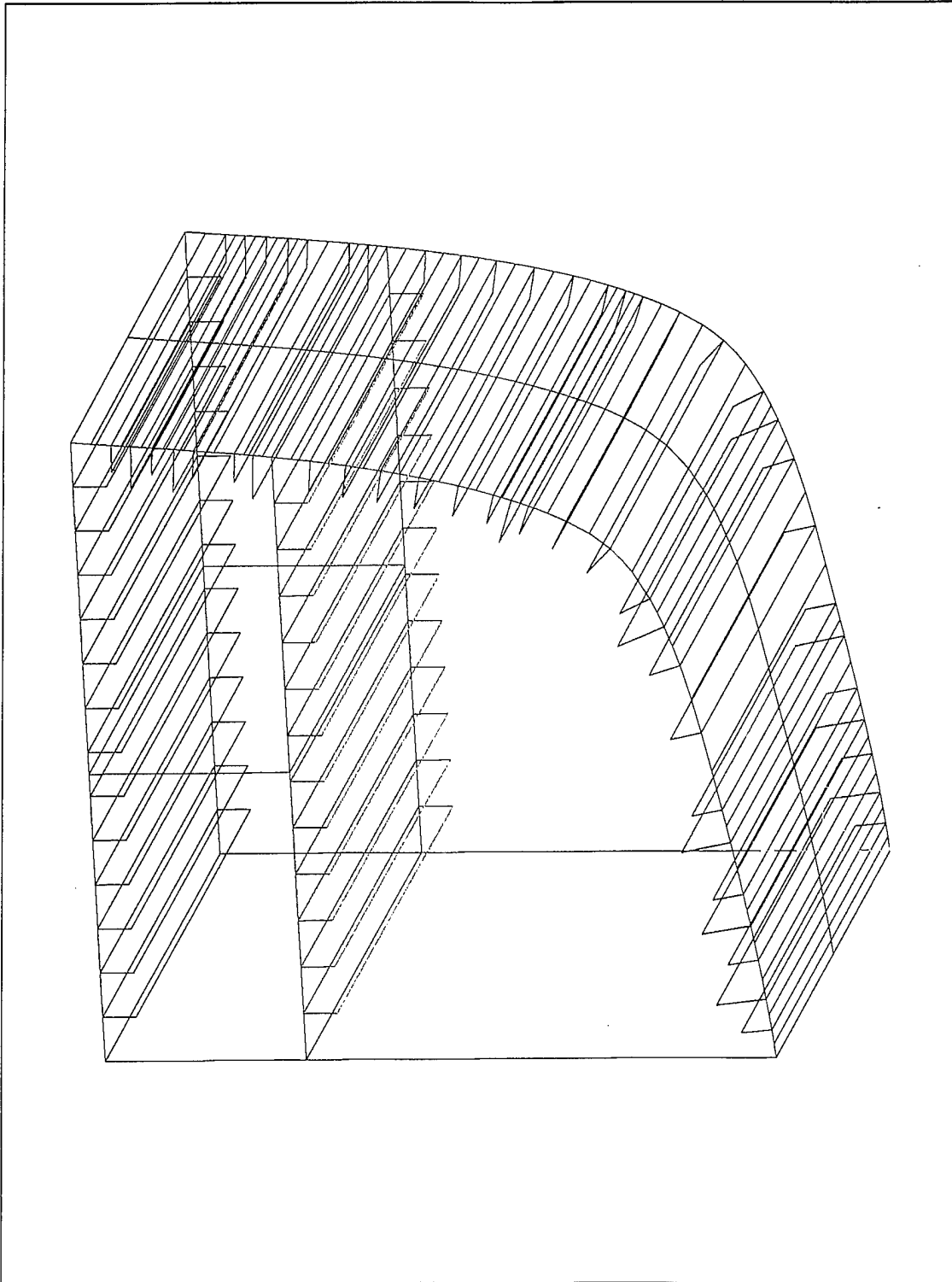


FIGURE 6. Isometric View of the Longitudinal Bulkhead Model's Surfaces and Reference Planes

the model solution. The user controls both the thickness of each element and the physical properties of each. The thickness and physical properties of each thin shell element in this study matched those of the design values of the FFG-7.

All longitudinal reinforcing in each section was simulated using beam elements. Beam elements were used in order to reduce the size and complexity of the mathematical model. The advantages of beam elements are that they reduce the number of nodes per element while still maintaining six degrees of freedom and maintaining the physical properties of the material being modeled. Furthermore, beam elements support static structural linear analyses. I-DEAS<sup>TM</sup> offers the additional advantage of storing a large number of commonly used reinforcing structures such as "T" beams in its beam element catalog within the beam section task. Overall, the use of beam elements in this study significantly reduced the size of the mathematical models necessary while still maintaining excellent accuracy in the solutions. Table 4 lists the number of nodes and elements for each model.

<b>ENTITY</b>	<b>HULL PENETRATION MODEL</b>	<b>LONGITUDINAL BLKHD MODEL</b>
Number of Nodes	3041	3645
Number of Elements	3836	4598

Table 4. Number of Nodes and Elements for Hull Penetration and Longitudinal Bulkhead Finite Element Models.

Since this study assumes simple beam bending theory in its development, an additional meshing procedure was deemed necessary. In order to keep initially plane sections plane after bending, rigid elements were placed at the centroids of the section areas where boundary conditions were to be specified. The use of rigid elements in these models implies that the motion of all the nodes on the element are related to each other as if they were connected by infinitely rigid, massless beams. The rigid elements were utilized on the fore and aft ends of each section. A node was placed at the centroid of the each section and was connected to every node in its vertical plane. The advantages this

provided were that a boundary condition could be placed at a single point in a plane and the plane would remain plane after bending. Lastly, the use of rigid elements supported this model by being applicable to static structural linear analyses and maintaining six degrees of freedom per node. Figures 7, 8, and 9 show the hull penetration model fully meshed from different aspects. Figures 10 and 11 depict the fully meshed longitudinal bulkhead model.

After the meshes were generated, quality checks on each mesh were accomplished. I-DEAS™ supports a number of quality checks that can prevent serious analysis errors. Each model was checked for erroneous free edges, coincident nodes, coincident elements, and distorted elements. All checks were satisfactory.

The distorted element check measured the element's deviation from its ideal shape. The range of possible distortion values is  $-1.0 \leq d \leq 1.0$  with 1.0 having no distortion. The accepted minimum distortion value for a critical analysis using I-DEAS™ is 0.7 [Ref. 10]. Every element in both models was found to have a distortion value of 0.7 or greater.

### C. BOUNDARY CONDITIONS

Boundary conditions were developed for this study from the bending moment curve of the FFG-7. The FFG-7 bending moment curve was generated assuming a full load displacement while positioned statically atop a trochoidal wave of height  $1.1\sqrt{L}$  in a hogging condition. Data points were taken from the bending moment curve and re-plotted using Matlab software. A polynomial generating function within Matlab was used to determine a polynomial representation of the curve. Equation (12) was the third-degree polynomial generated.

$$M(x) = (1E+08) [ (-5.941E-09)x^3 + (2.790E-05)x^2 - \dots \\ (0.02812)x + (9.9128) ] \quad \text{Equation (12)}$$

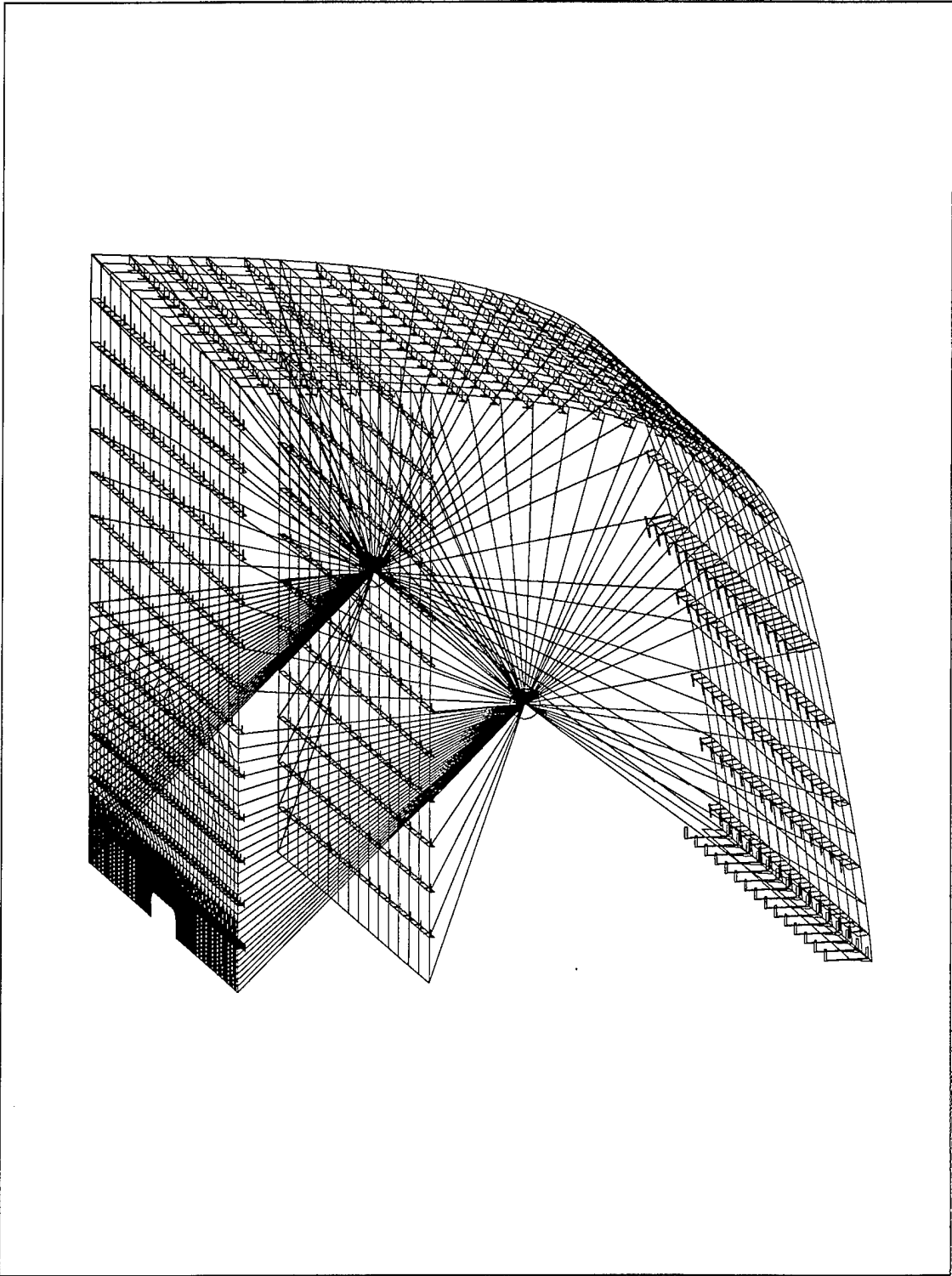


FIGURE 7. Fully Meshed Hull Penetration Model with Beam and Rigid Elements

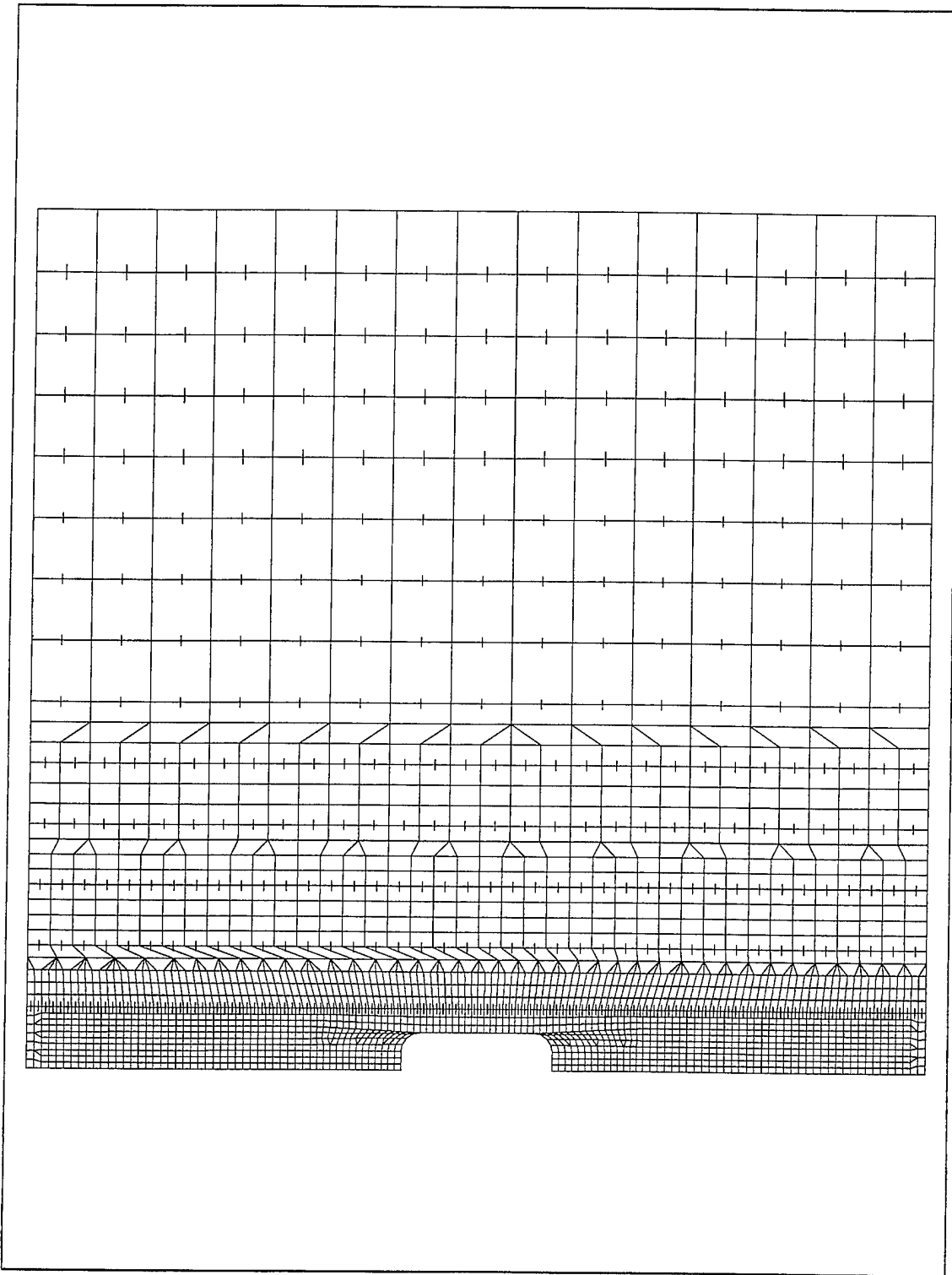


FIGURE 8. Fully Meshed Main Deck of Hull Penetration Model

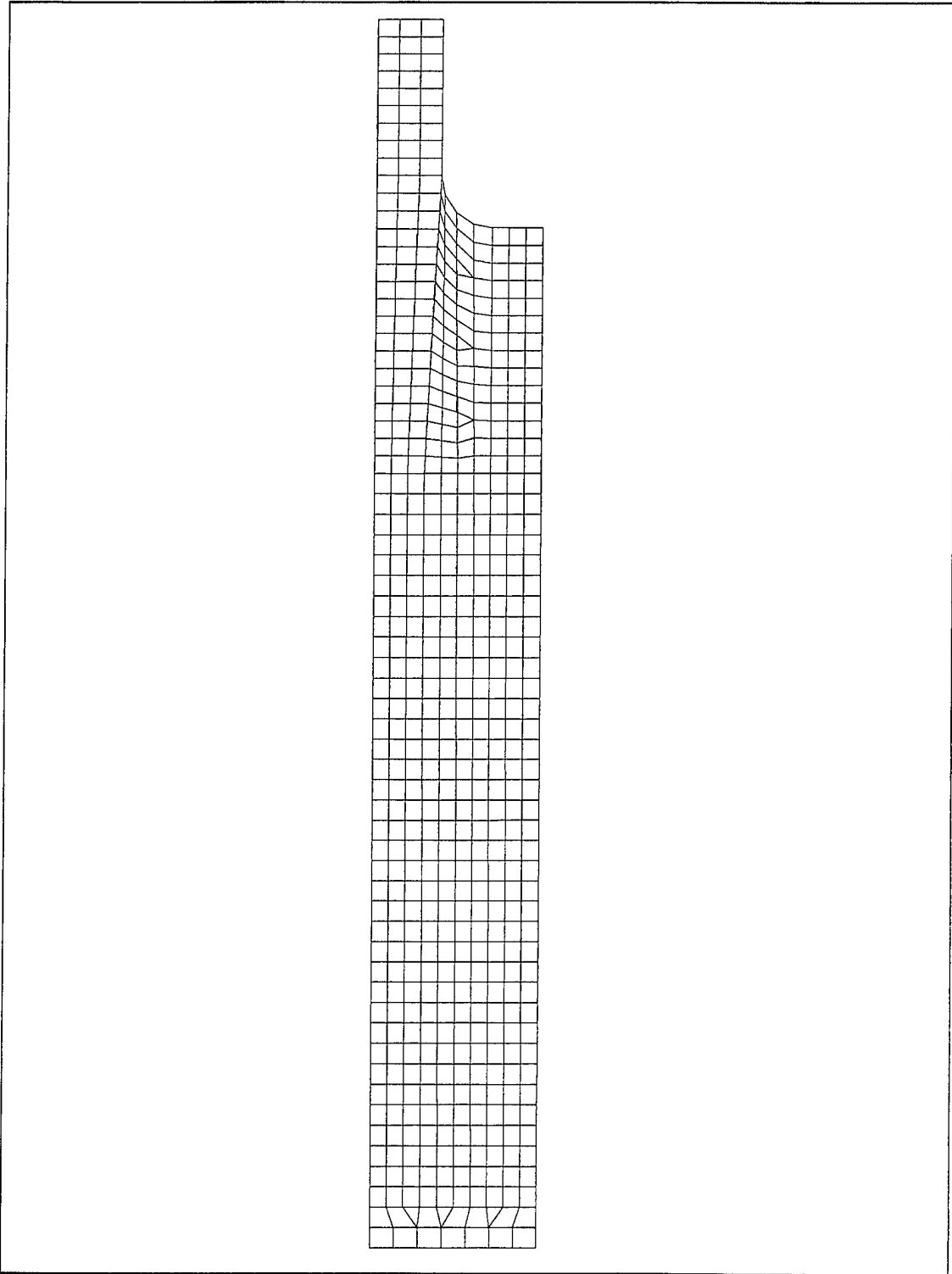


FIGURE 9. Meshed Surface Around Hull Penetration in Hull Penetration Model

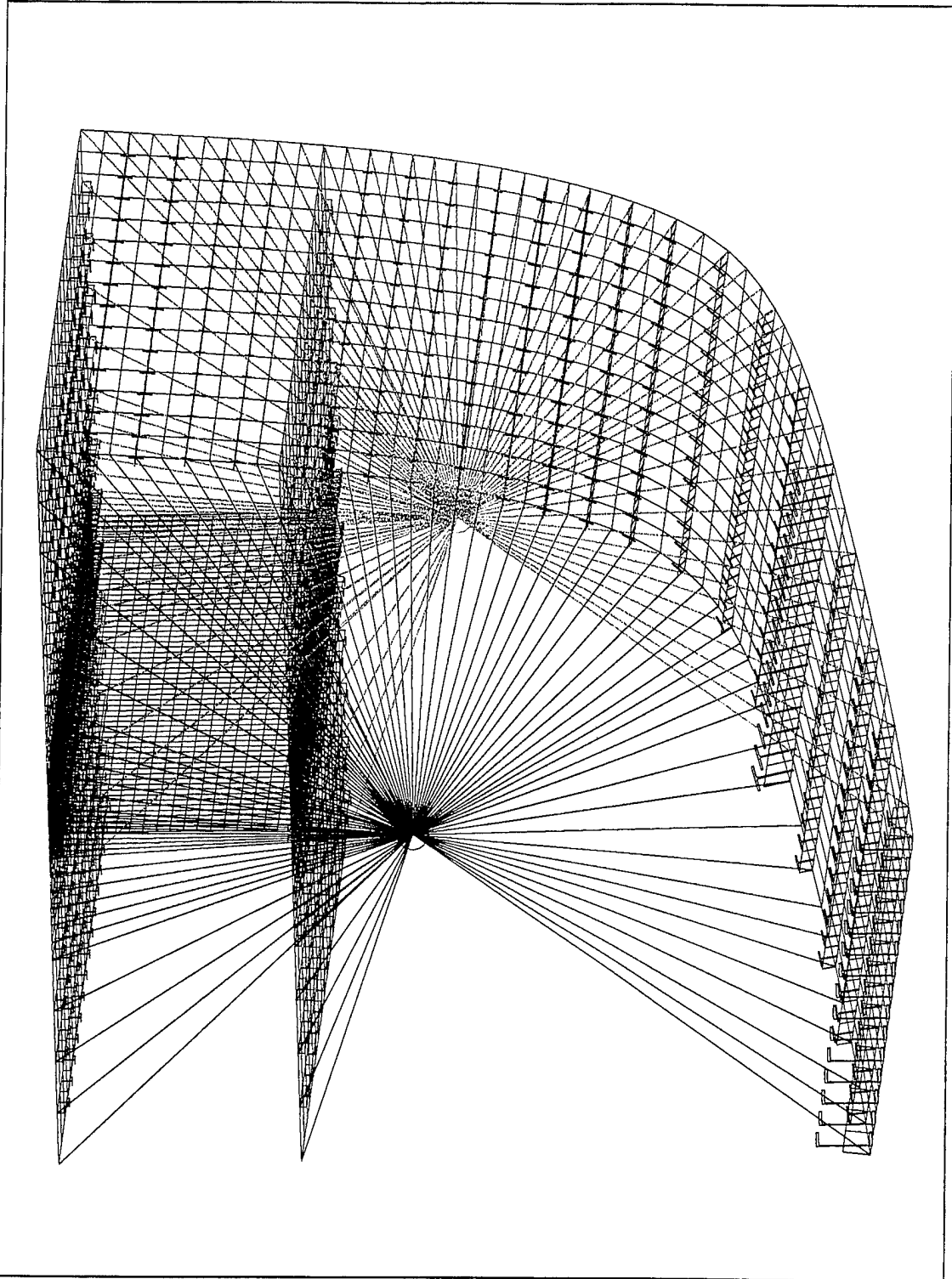


FIGURE 10. Fully Meshed Surfaces of Longitudinal Bulkhead Model with Beam and Rigid Elements

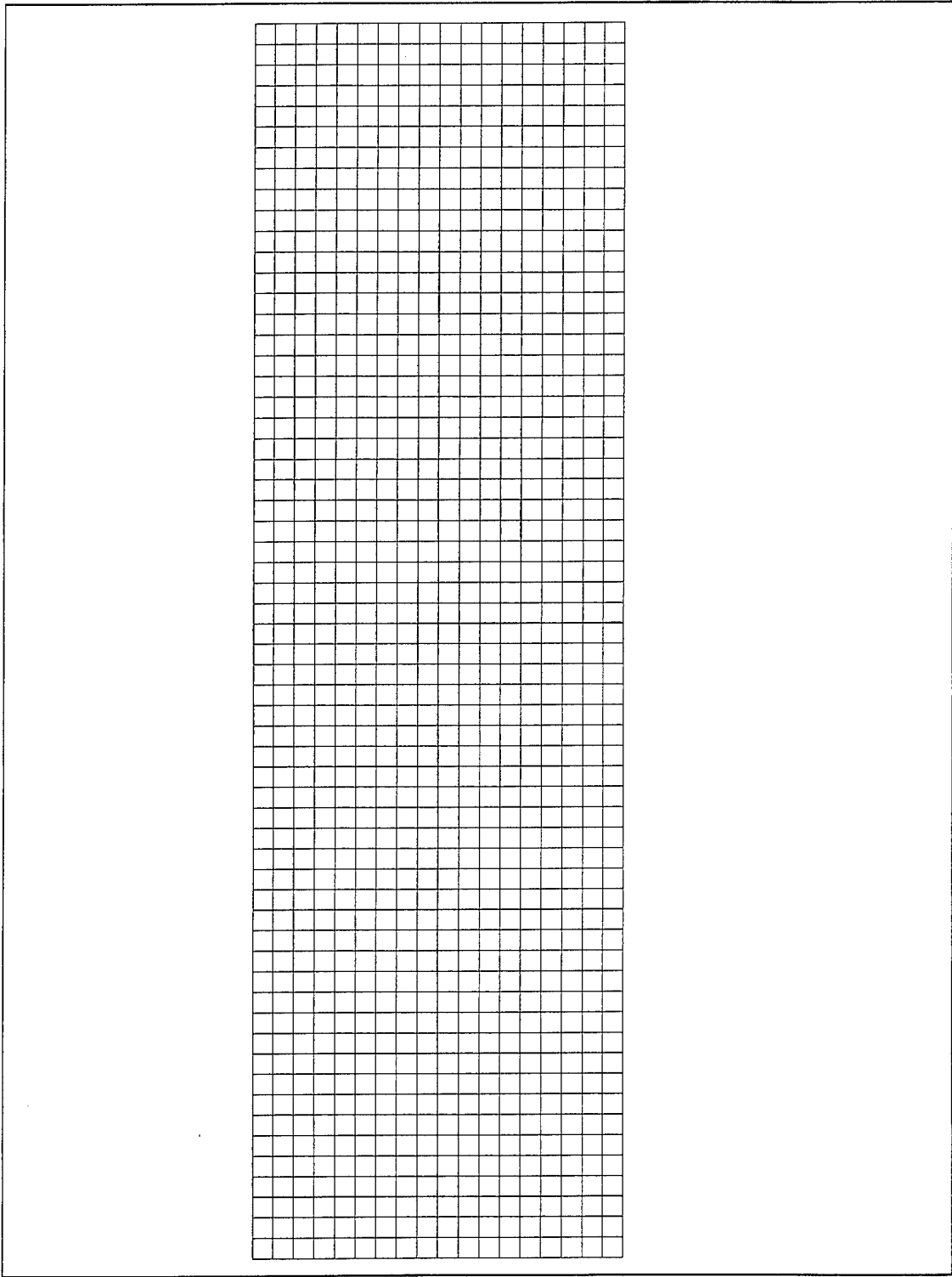


FIGURE 11. Meshed Surface of Longitudinal Bulkhead in the Longitudinal Bulkhead Model

Applying simple beam bending theory and Equation (7), Equation (12) was integrated with respect to length to obtain the slope. The resulting equation was integrated using Equation (8) to determine the hull displacement as a function of length. Both the slope and displacement for the section being studied were determined under the assumption that the section modulus remained constant over the 30 foot section. The actual FFG-7 section modulus decreases by slightly less than 1% in that area. However, since this study assumed a constant section modulus it was appropriate to calculate the slope and displacement in this manner vice using the actual section modulus values. Table 5 lists the calculated displacement and slope 30 feet in the longitudinal direction from station 10. The results are relative to station 10.

Displacement	-0.0172 ft.
Slope	1.075E-03 radians

Table 5. Boundary Conditions Calculated from FFG-7 Bending Moment Curve 30 Feet from Station 10 and Relative to Station 10.

A comparison was done to verify deflection results obtained from integrating the bending moment curve. The deflection calculated at station 10 relative to the end of the ship was compared to the deflection calculated from Equation (13).

$$v = k \frac{ML^2}{EI} \quad \text{Equation (13)}$$

where:

$M$  = Bending moment amidships

$L$  = Length of ship

$k$  = 0.09, a dimensionless constant

Equation (13) is a semi-empirical expression developed for calculating the overall hull deflection amidships for large vessels. [Ref. 11] The overall deflection at station 10 (midships) as determined through the bending moment integration was 6.32 inches, (relative to the hull ends). The deflection calculated from Equation (13) was 6.50 inches. The slight difference is attributed to the fact that the semi-empirical expression was developed from the history of a variety of vessels. Based on the similar results obtained, the expressions developed through integration of the bending moment curve were assumed correct. This provided confidence in the data used for the boundary conditions listed in Table 5.

The relative slope and displacement of the hull listed in Table 5 were applied as boundary conditions for both models. They were applied to the node that was located on the centroid of the cross section 30 feet from station 10. The node was further restrained by imposing a “clamped” condition on it. The “clamped” restraint fixed the six degrees of freedom on the centroidal node and the rigid elements attached to it. This follows from the assumption of plane sections remaining plane after bending. The same procedure was also used for the node located on the centroid of the section at station 10 except that the displacement and slope were zero. These values were zero since the boundary conditions in Table 5 were determined relative to station 10.

The other necessary boundary condition applied to both models was a restraint in the transverse direction. This accounted for the missing mirrored image of the section modeled. All of the boundary conditions were applied using the Boundary Conditions task within I-DEAS™. Figure 12 is a graphical depiction of the boundary conditions applied to the centroidal nodes and the geometry-based restraint applied in the transverse direction for the hull penetration model. The longitudinal bulkhead model has the same graphical depiction.

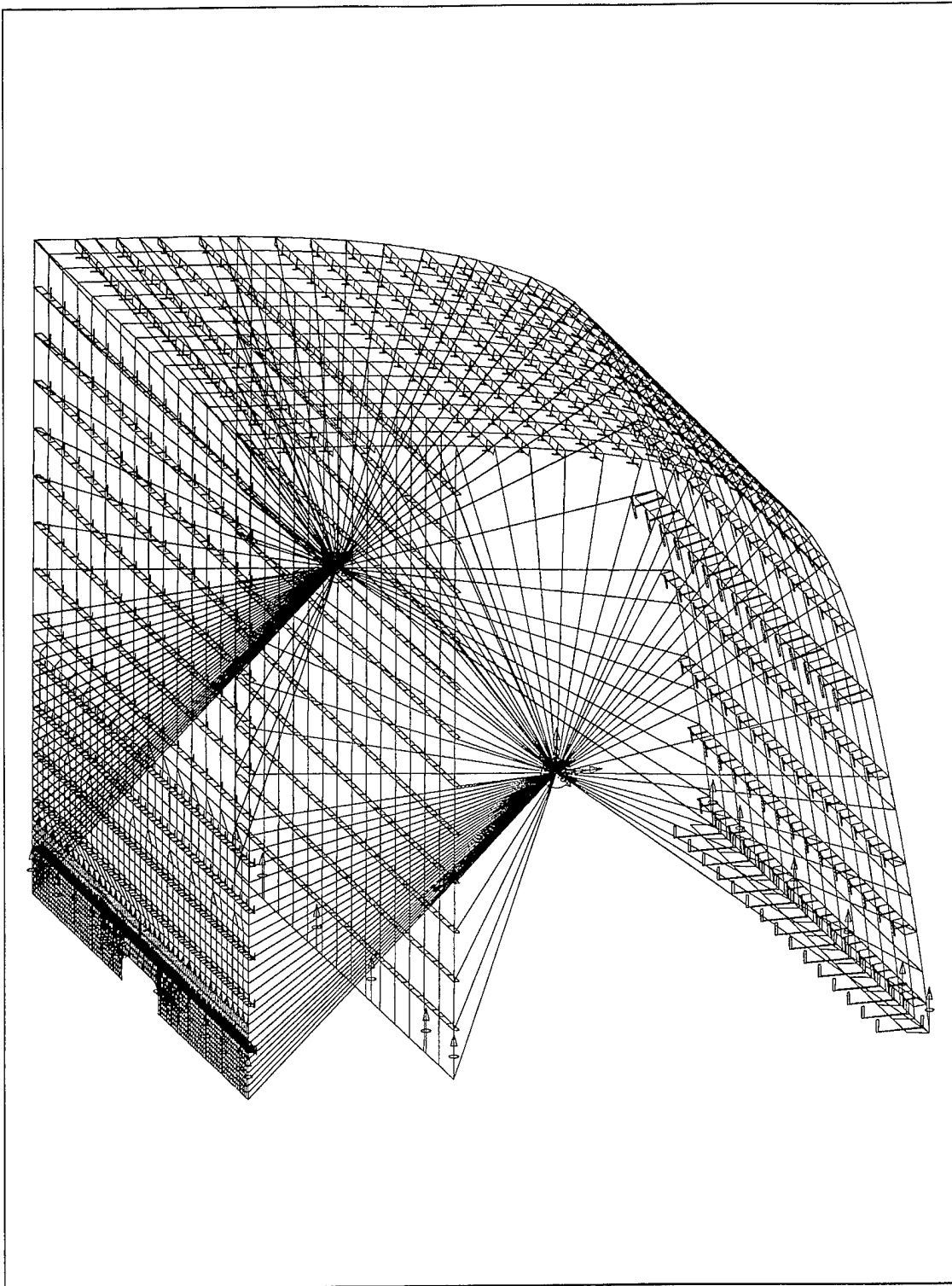


FIGURE 12. Meshed Surface with Boundary Conditions on the Hull Penetration Model



## IV. RESULTS

### A. HULL GIRDER PENETRATION MODEL

Figure 13 depicts the resulting Von Mises stress distribution for the hull penetration model. The deformed model shows bending similar to that of a beam bending under a distributed load. This was expected since the model was developed under the theory of simple beam bending. However, the hull penetration on the main deck caused an obvious disruption of the longitudinal stress distribution. As the rule of thumb for a hull penetration predicted, there is an area of lower stress immediately fore and aft of the penetration. The average stress in the lower stress regions is approximately 4.0 ksi whereas the average stress in the remainder of the main deck is approximately 14.5 ksi. (Figure 14) Between the two stress regions is a definitive transition zone which can be approximated to parallel a straight line.

Figure 15 is an exploded view of the stress transition area around the penetration. A line tangent to the penetration radius has been drawn on the colored plot. The line separates the area of high stress from that of the low stress. The exact placement of the line is somewhat judgment-based. However, the placement of this line in Figure 15 was drawn with a 1:4 slope as stated by the rule of thumb. As can be seen, this is a very good approximation for encompassing the area of significantly lower stress. Hence, the results here are considered to have validated the rule of thumb for a line with a 1:4 slope around the ineffective area.

In order to help prove the validity of the model, results were compared to known data for the exact same loading condition. At station 10 for the hogging condition specified, the known maximum stress in the main deck is 15.1 ksi [Ref. 12]. This compares to a value of 15.2 ksi from the model. The value of 15.2 ksi was taken from the center area of the main deck and sufficiently far enough away from the stress

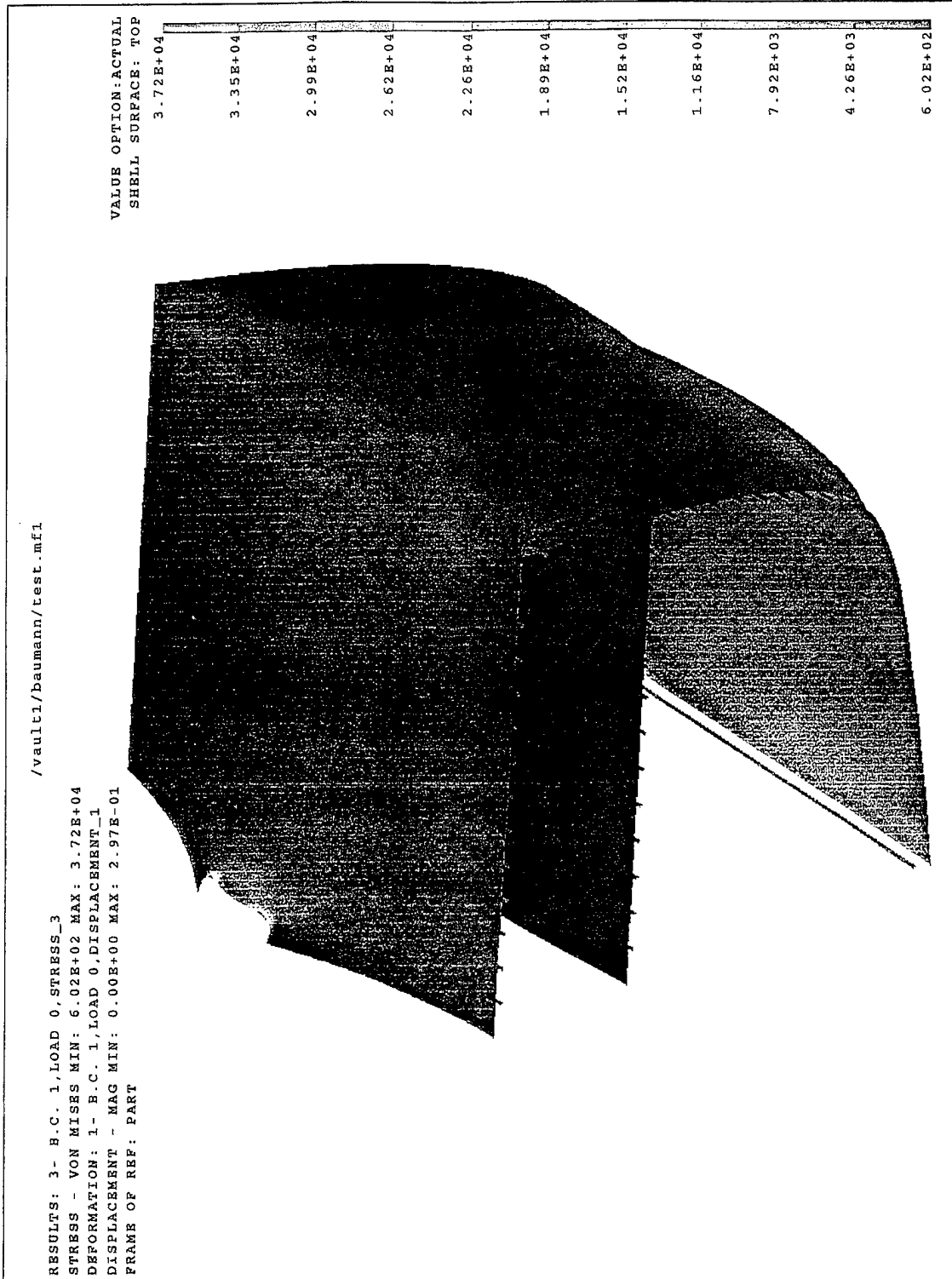


FIGURE 13. Stress Distribution for the Deformed Hull Penetration Model (ksi)

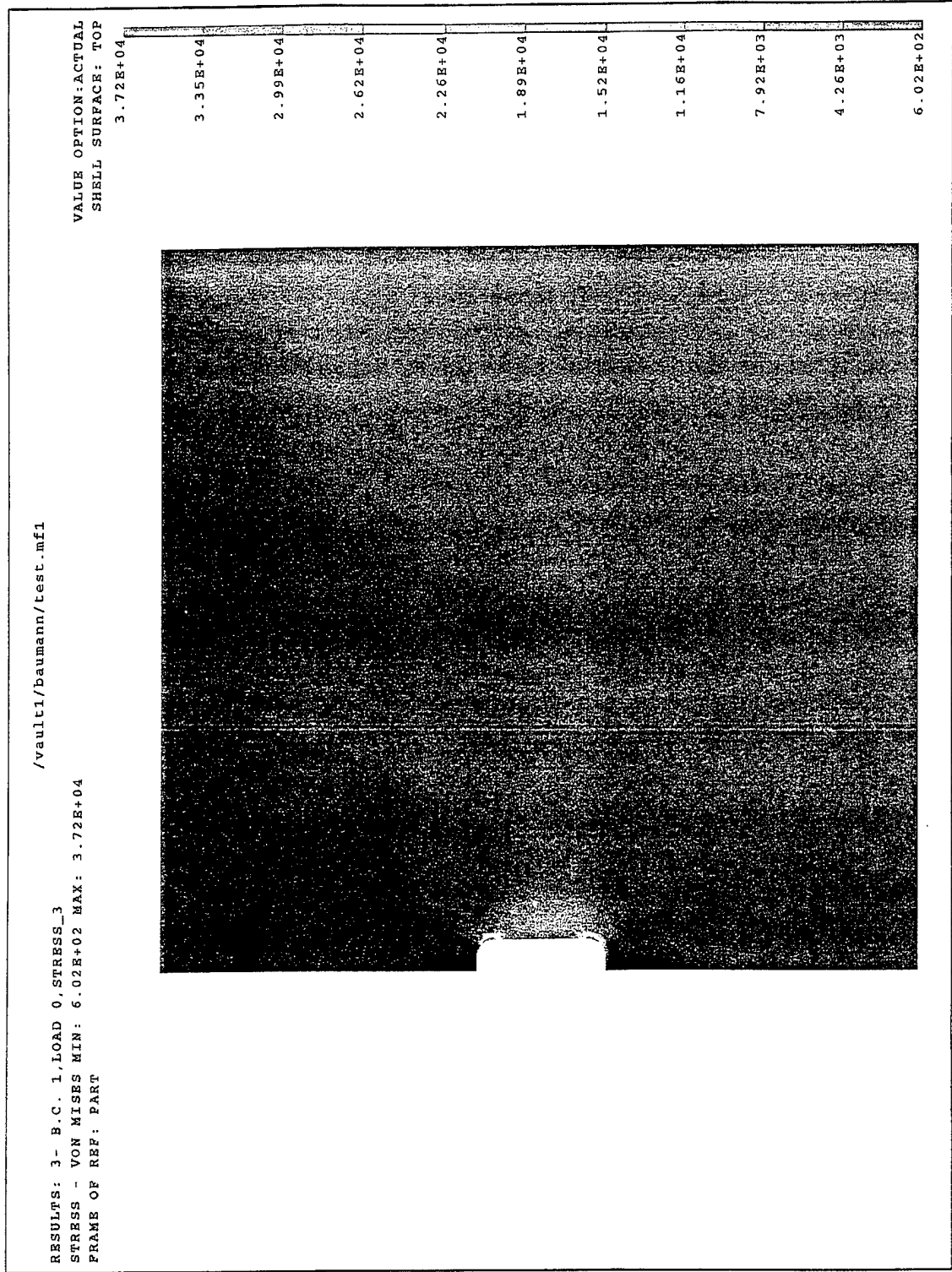


FIGURE 14. Stress Distribution on Main Deck of Hull Penetration Model (ksi)

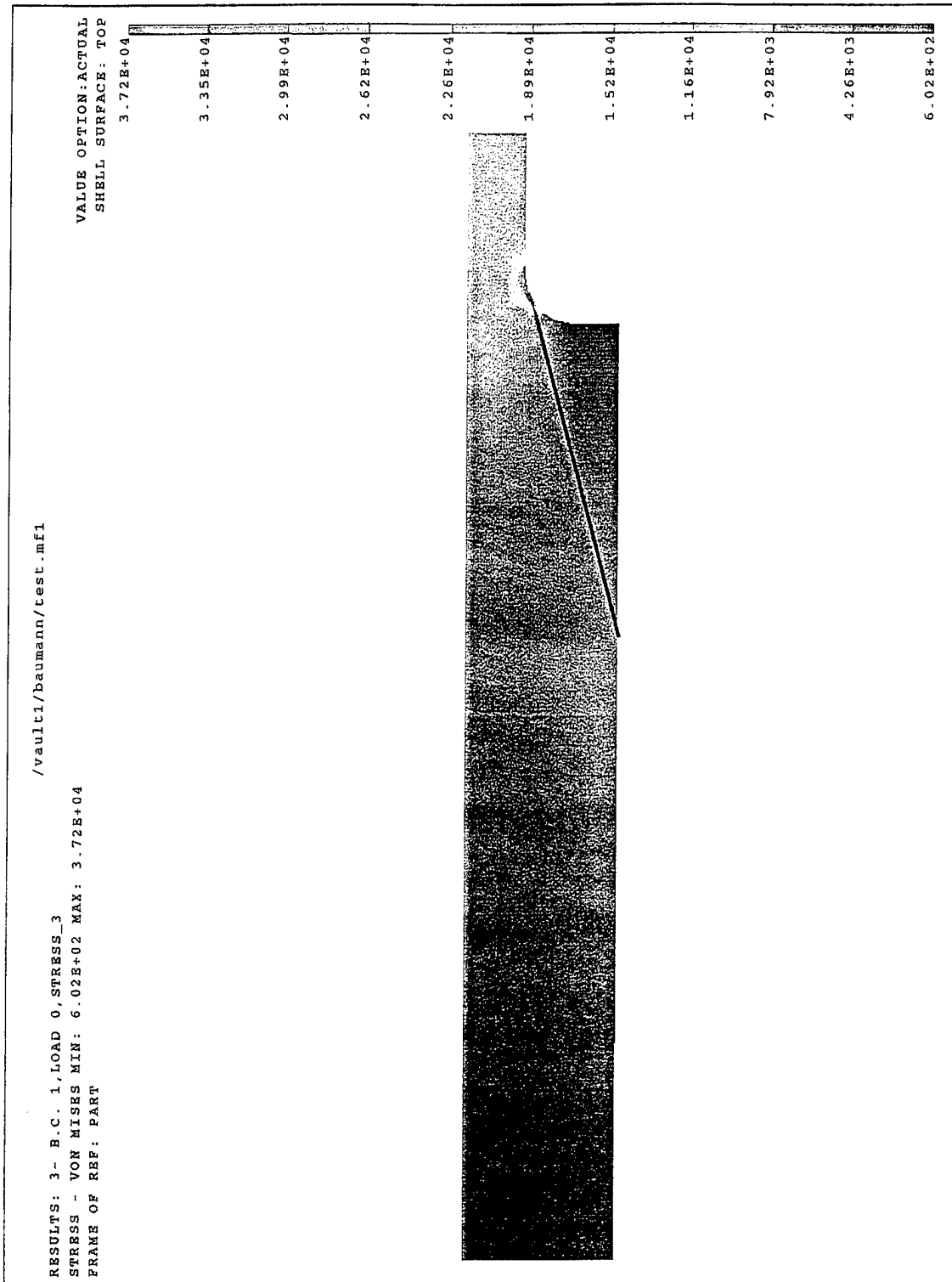


FIGURE 15. Exploded View of Stress Distribution Around the Hull Penetration (ksi)

concentrations to allow for a comparison. The difference between the two values is less than 1%.

Two additional comparisons were made to help validate the results. The first compared the locations and value of peak stress around the penetration of the main deck. Gibzstein predicts that this value can be approximated by the empirical relationship in Equations (14) and (15) for stress concentrations around rectangular openings in a plate in tension [Ref. 13]. Although Gibzstein's relationship is for pure tension, it can be used as an approximation here since this model has such a small deflection over its entire span that the deck is, effectively, in pure tension. This means that the resulting bending stresses in the thin shell act as forces in tension in a thin flat plate.

$$k = \frac{1 - 0.4^{B/b}}{2 - 0.4^{l/B}} \left[ 1 + \frac{0.926}{1.348 - 0.826^{20r/B}} \left( 0.577 - \left( \frac{b}{B} - 0.24 \right)^2 \right) \right] \quad \text{Equation (14)}$$

$$\sigma_{\max} = k\sigma_{\text{avg}} \quad \text{Equation (15)}$$

where:

$k$  = stress concentration factor

$B$  = width of the plate

$b$  = width of rectangular penetration

$r$  = radius of the corners of the penetration

$l$  = length of the penetration

The second comparison only compares the value of peak stress around the penetration. Peterson provides graphical predictions for a range of penetration dimensions in a flat plate under uniaxial tension. Values for penetration length, width, and corner

radius are applied to the graph and the resulting stress concentration factor is determined.  
[Ref. 14]

Gibzstein predicts the peak stress concentration to be 32.2 ksi. The results in the model show a stress concentration of 37.2 ksi. This equates to a 13.4% difference. In addition, Gibzstein predicts the stress concentration to be approximately 5-10 degrees from the start of the radius on the side parallel to the longitudinal axis. Peterson, in comparison, predicts the peak stress concentration to be 42.3 ksi. This equates to a 13.7% difference. The difference between the two predictions can be attributed to Gibzstein's model accounting for plate width whereas Peterson assumes an infinite width. The resulting peak stress concentration of this model is approximately equal to the average of the two predictions. Hence, this model's data correlates well with the predicted value.

## **B. LONGITUDINAL BULKHEAD MODEL**

Figure 16 depicts the Von Mises stress distribution of the deformed longitudinal bulkhead model while Figure 17 is an exploded view of the bulkhead itself. Clearly, there are two distinctive stress level regions across the bulkhead. The average stress in the upper section of the bulkhead is approximately 14.0 ksi and transitions to the value of stress in the main deck. The average stress in the lower zone of the bulkhead near the vertical edges on the end is 3.0 ksi.

Similar to what the rule of thumb for a short longitudinal bulkhead predicted, there is a well defined separation between the area of higher stress concentration and that of the lower concentration. As was the case in the previous model, a line can be drawn separating the two regions and paralleling the transition zone. The exact placement of the line is somewhat judgment-based. However, the placement of the line in Figure 17 was drawn with a 1:4 slope as stated by the rule of thumb. As can be seen, this is a very good

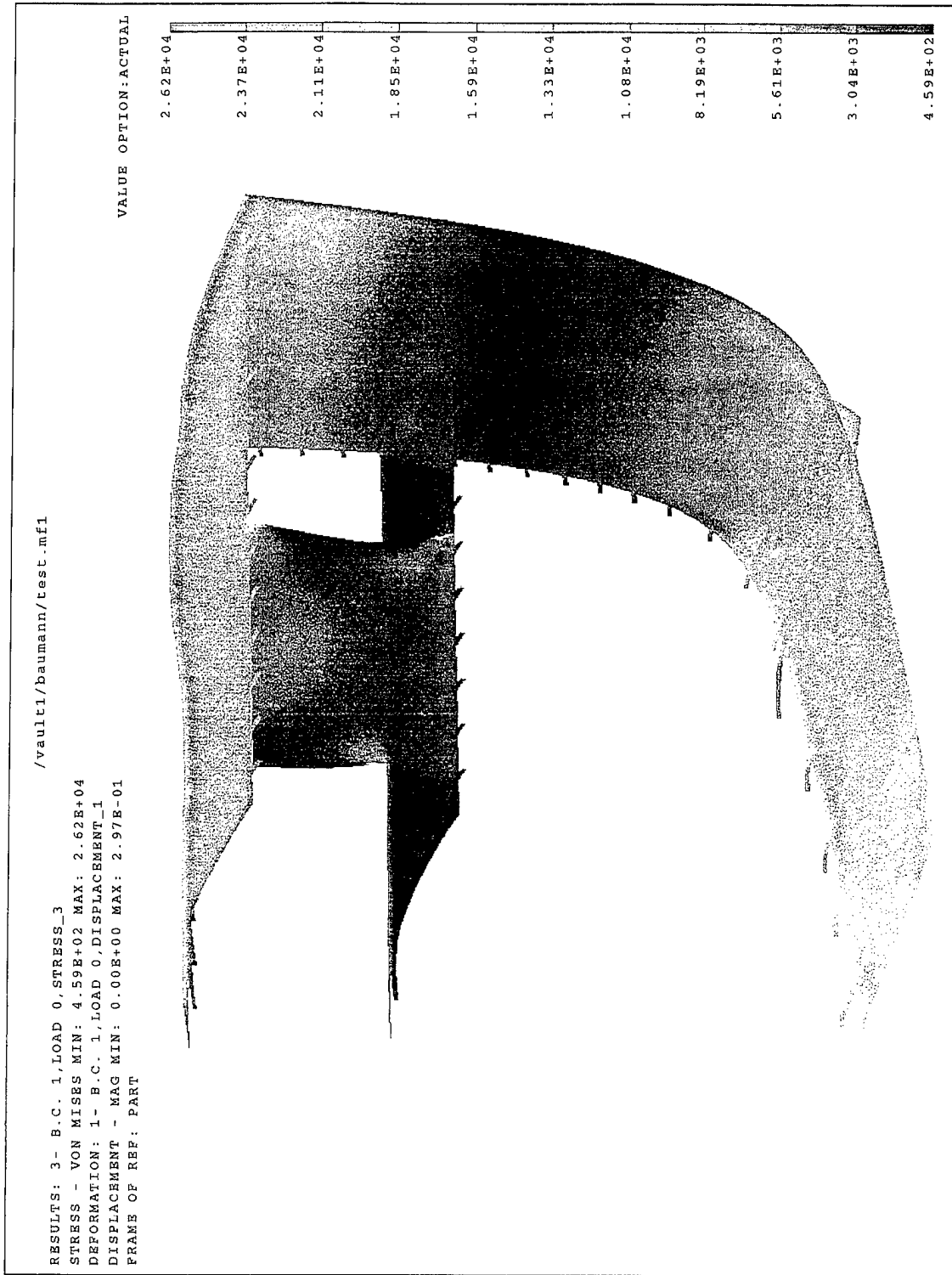


FIGURE 16. Stress Distribution for Deformed Longitudinal Bulkhead Model (ksi)

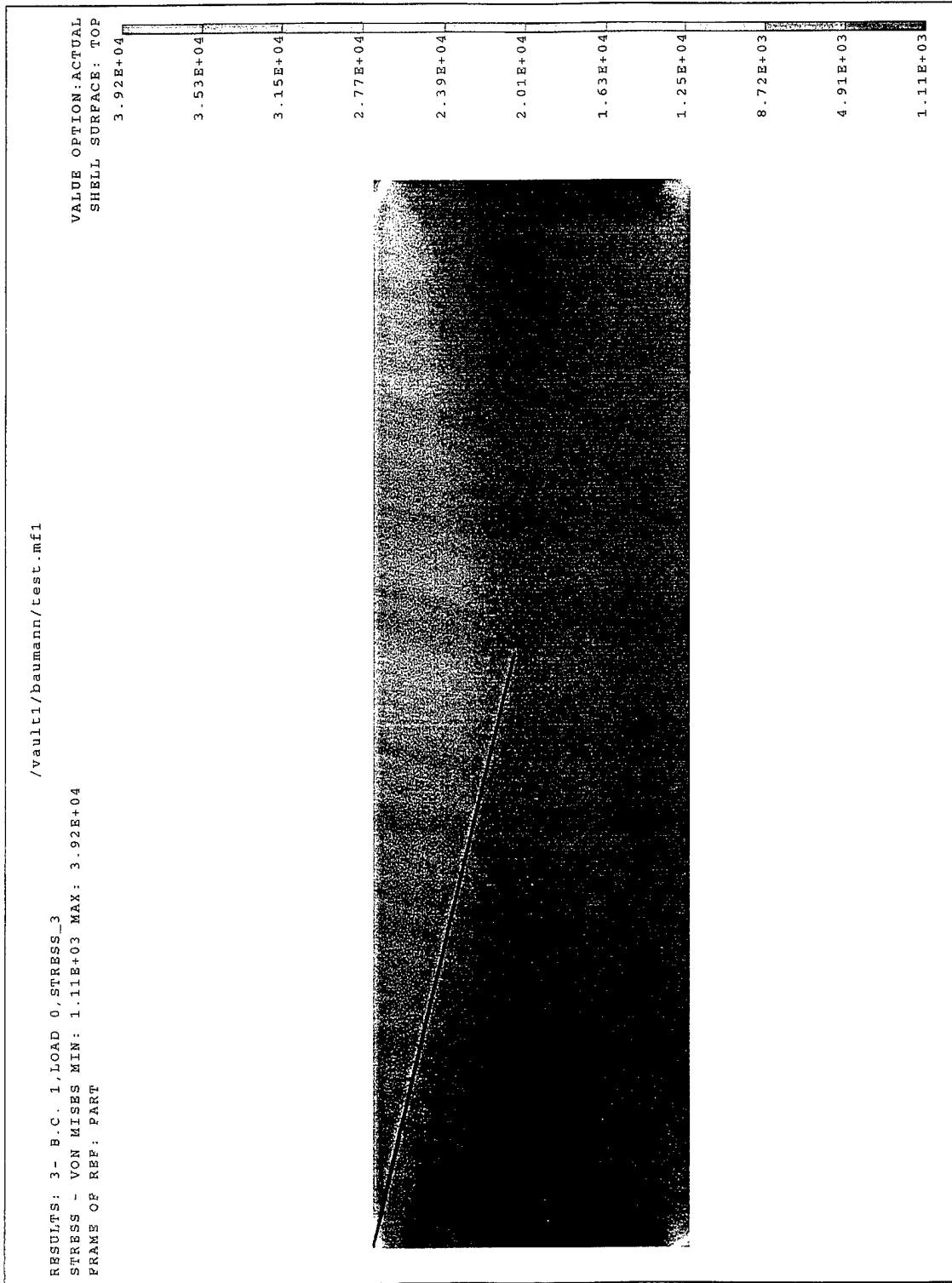


FIGURE 17. Stress Distribution on Longitudinal Bulkhead (ksi)

approximation for isolating the area of significantly lower stress and validates the assumption of the line having a 1:4 slope.

Also distinguishably noticeable are peak stress concentrations in the four corners of the bulkhead. This was caused by the fact that there were only 2 discrete and finite points on each end of the bulkhead in the vertical plane that were attached to the boundary conditions. When the boundary conditions were applied, peak stress concentrations were created at those points. The stress was then distributed to the surrounding bulkhead material. This is evident by the fanning out of the stress concentration in each corner.

The rule of thumb for short longitudinal bulkheads also predicts a similar transition region emanating from the lower corners of the bulkhead. However, in this model the resulting stress in the middle deck is approximately 4.0 ksi. Since the stress in the middle deck is similar in value to that of the stress in the ineffective area of the bulkhead, there is no reason for a transition region. Hence, a line originating from the lower corner of the bulkhead cannot be drawn.

### **C. MODELING PROCEDURES**

The mathematical models developed for this study were done using sound engineering principles and assumptions. They were applied to the I-DEAS<sup>TM</sup> software under the guiding principles provided in the software's documentation while also incorporating standard finite element analysis theory [Ref. 15]. In addition, mesh refinement procedures were used throughout the study to obtain data convergence. Lastly, an overall assessment of the entire study was done using the evaluation criteria presented in "Guideline for Evaluation of Finite Elements and Results" [Ref. 16]. This technical report was developed for the Ship Structure Committee which is comprised of the following member agencies. (Figure 18)

American Bureau of Shipping  
Defence Research Establishment Atlantic  
Maritime Administration  
Military Sealift Command  
Naval Sea Systems Command  
Transport Canada  
United States Coast Guard

FIGURE 18. Ship Structure Committee Member Agencies

The report was designed to be used as a tool in assessing the applicability and validity of finite element models as applied to the ship design industry. It provides a detailed and exhaustive checklist covering all aspects of finite element modeling. Figure 19 shows the overall evaluation methodology suggested in the report while the detailed breakdown of each category can be found in Reference [16]. The analysis described herein was evaluated using this checklist, and it was determined that it satisfactorily met the requirement criteria for an "Acceptable" finite element analysis.

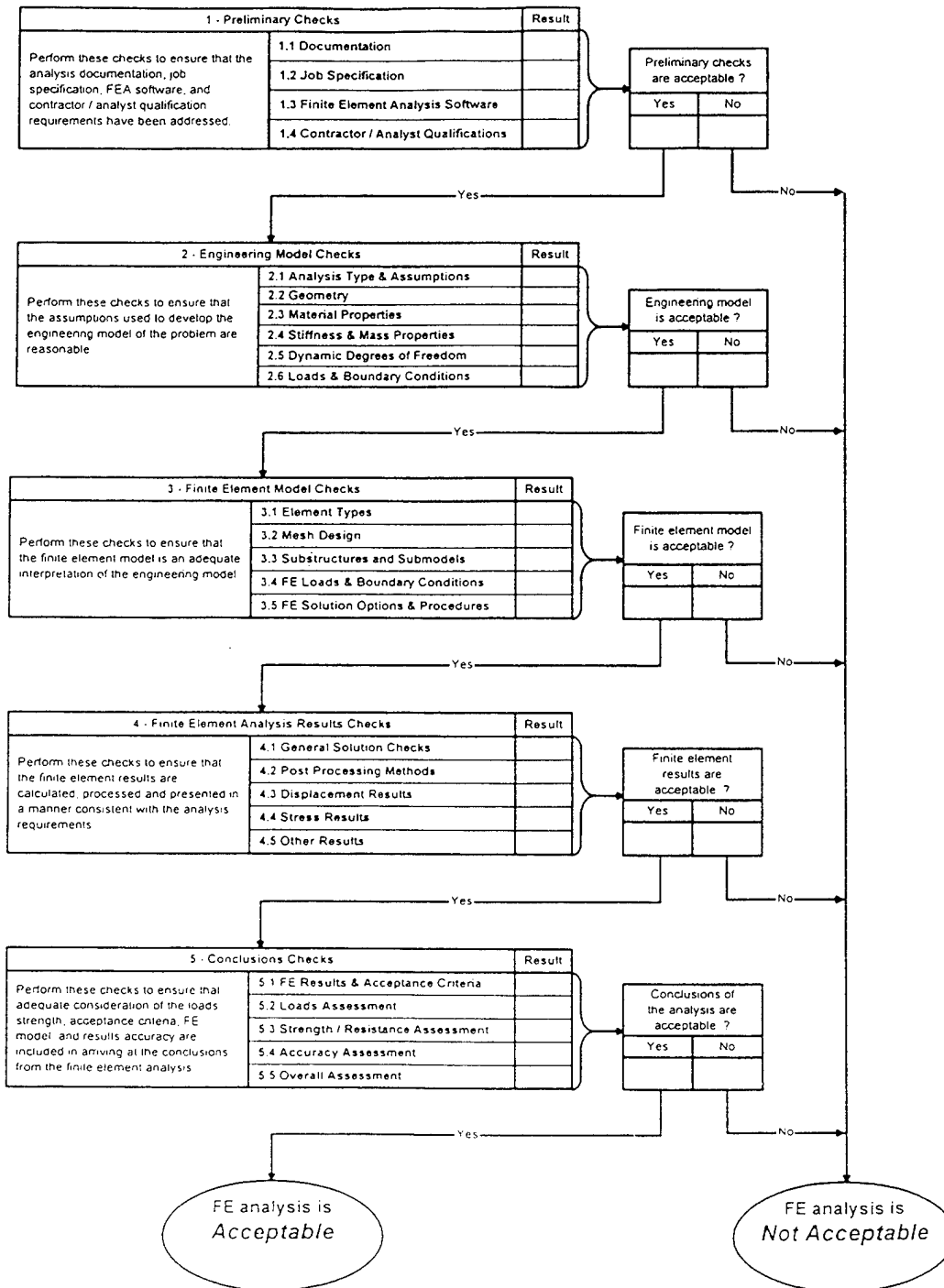


FIGURE 19. Overall Finite Element Model Evaluation Methodology Chart



## V. CONCLUSIONS

This study applied powerful finite element analysis software in analyzing the stress distributions resulting from two different structural situations. First, it analyzed the shadow zone resulting from placing a standard size personnel access cut in the main deck of a U.S. Navy Oliver Hazard Perry Class Guided Missile Frigate (FFG-7). Next, it analyzed the shadow zone resulting from placing a short structural longitudinal bulkhead in the same hull. In both cases, a finite element model was developed using the actual hull design as a reference.

The finite element models were developed and analyzed using the I-DEAS<sup>TM</sup> finite element software. A static linear analysis was done using the boundary conditions resulting from balancing the FFG-7 hull on a trochoidal wave of height  $1.1\sqrt{L}$ . Thin shell linear quadrilateral and triangular elements coupled with beam and rigid elements were used in forming the meshes. A mapped mesh was used in order to have better control over mesh density.

Resulting Von Mises stress distributions were plotted using colored stress plots. In both cases, an area of lower stress concentration resulted as predicted by the rules of thumb. The hull penetration model clearly showed an area of low stress immediately fore and aft of the access cut. The stress distribution and associated stress transition area was such that a line could be drawn along the transition area that separated the area of high stress from that of low stress. The line was drawn tangent to the radius of the corner of the penetration and intersected the centerline of the hull on the main deck. This line had a slope of 1:4.

In the short longitudinal bulkhead model, an area of lower stress concentration was present immediately adjacent to either end of the bulkhead. As in the other model, a line could be drawn along the transition area that separated the two regions of varying stress.

The line, originating from the upper corner of the bulkhead, was drawn with a downward angle towards the center of the bulkhead. This line also had a slope of 1:4.

The results of this study confirm the accuracy of the rules of thumb for hull girder penetrations and short longitudinal bulkheads. The development of the models was intended to be generic enough to allow the results to have wide applicability while still using data from an actual hull form. The results of the study shouldn't be used as guidance for a final design since a design may have other factors contributing to the stress distribution. However, they can be applied with confidence when used as a quick reference in preliminary designs.

## LIST OF REFERENCES

1. *The Manual for Naval Surface Ship Design Technical Practices*, Chap. VIII, United States Naval Sea Systems Command, 1974.
2. Bartholomew, C., Marsh, B., Hooper, R., *U.S. Navy Salvage Engineer's Handbook*, vol. 1, United States Naval Sea Systems Command, May 1992.
3. Bartholomew, C., Marsh, B., Hooper, R., *U.S. Navy Salvage Engineer's Handbook*, vol. 1, United States Naval Sea Systems Command, May 1992.
4. Taggart, R., *Ship Design and Construction*, The Society of Naval Architects and Marine Engineers, 1980.
5. Rawson, K., Tupper, E., *Basic Ship Theory*, vol. 1, Longman, 1983.
6. "I-DEAS<sup>TM</sup> Course Guide, The Analysis Course," *I-DEAS<sup>TM</sup> Master's Series*, Structural Dynamics Research Corporation, 1996.
7. Lawry, M., "I-DEAS<sup>TM</sup> Student Guide," *I-DEAS<sup>TM</sup> Master's Series*, Structural Dynamics Research Corporation, 1993.
8. *Specifications for Building Guided Missile Destroyer DDG 52 and Follow*, vol. II, United States Naval Sea Systems Command, 26 May 1987.
9. Lawry, M., "I-DEAS<sup>TM</sup> Student Guide," *I-DEAS<sup>TM</sup> Master's Series*, Structural Dynamics Research Corporation, 1993.
10. "I-DEAS<sup>TM</sup> Course Guide, The Analysis Course," *I-DEAS<sup>TM</sup> Master's Series*, Structural Dynamics Research Corporation, 1996.
11. Taggart, R., *Ship Design and Construction*, The Society of Naval Architects and Marine Engineers, 1980.
12. Bartholomew, C., Marsh, B., Hooper, R., *U.S. Navy Salvage Engineer's Handbook*, vol. 1, United States Naval Sea Systems Command, May 1992.
13. M. Gibzstein, "Maximum Stress Concentration at Rectangular Openings with Rounded Corners in Plates of Finite Dimensions," *European Shipbuilding*, 1965.
14. Peterson, R. E., *Stress Concentration Factors*, Wiley-Interscience, 1974.

15. Lawry, M., "I-DEAS<sup>TM</sup> Student Guide," *I-DEAS<sup>TM</sup> Master's Series*, Structural Dynamics Research Corporation, 1993.
16. *Guideline for Evaluation of Finite Elements and Results*, SSC-387, Ship Structure Committee, 1996.

## INITIAL DISTRIBUTION LIST

	No. Copies
1. Defense Technical Information Center . . . . . 8725 John J. Kingman Rd., STE 0944 Ft. Belvoir, Virginia 22060-6218	2
2. Dudley Knox Library . . . . . Naval Postgraduate School 411 Dyer Rd. Monterey, CA 93943-5101	2
3. Chairman, Code ME . . . . . Department of Mechanical Engineering Naval Postgraduate School Monterey, CA 93943-5000	1
4. Professor Charles Calvano, ME/Ca . . . . . Department of Mechanical Engineering Naval Postgraduate School Monterey, CA 93943-5000	2
5. Professor Josh Gordis, ME/Go . . . . . Department of Mechanical Engineering Naval Postgraduate School Monterey, CA 93943-5000	2
6. LT G. W. Baumann, USN . . . . . 711 Old Lane Rd. Vestal, NY 13850	2
7. Executive Director . . . . . Ship Structure Committee U.S. Coast Guard (G-M) 2100 Second Street, S.W. Washington, D.C. 20593-0001	1